CellPress
Partner Journal

Molecular Plant
Research article

Cell-type-specific transcriptomics reveals that root hairs and endodermal barriers play important roles in beneficial plant-rhizobacterium interactions

Eline H. Verbon[1,5], Louisa M. Liberman[2,3,5], Jiayu Zhou[1], Jie Yin[1], Corné M.J. Pieterse[1], Philip N. Benfey[2,3], Ioannis A. Stringlis[1,4,*] and Ronnie de Jonge[1,*]

[1]Plant-Microbe Interactions, Department of Biology, Science4Life, Utrecht University, P.O. Box 800.56, 3508 TB Utrecht, the Netherlands

[2]Howard Hughes Medical Institute, Duke University, Durham, NC 27708, USA

[3]Department of Biology, Duke University, Durham, NC 27708, USA

[4]Laboratory of Plant Pathology, Agricultural University of Athens, 75 Iera Odos str., 11855 Athens, Greece

[5]These authors contributed equally to this article.

***Correspondence: Ioannis A. Stringlis (i.stringlis@aua.gr), Ronnie de Jonge (r.dejonge@uu.nl)**

https://doi.org/10.1016/j.molp.2023.06.001

ABSTRACT

Growth- and health-promoting bacteria can boost crop productivity in a sustainable way. *Pseudomonas simiae* WCS417 is such a bacterium that efficiently colonizes roots, modifies the architecture of the root system to increase its size, and induces systemic resistance to make plants more resistant to pests and pathogens. Our previous work suggested that WCS417-induced phenotypes are controlled by root cell-type-specific mechanisms. However, it remains unclear how WCS417 affects these mechanisms. In this study, we transcriptionally profiled five *Arabidopsis thaliana* root cell types following WCS417 colonization. We found that the cortex and endodermis have the most differentially expressed genes, even though they are not in direct contact with this epiphytic bacterium. Many of these genes are associated with reduced cell wall biogenesis, and mutant analysis suggests that this downregulation facilitates WCS417-driven root architectural changes. Furthermore, we observed elevated expression of suberin biosynthesis genes and increased deposition of suberin in the endodermis of WCS417-colonized roots. Using an endodermal barrier mutant, we showed the importance of endodermal barrier integrity for optimal plant-beneficial bacterium association. Comparison of the transcriptome profiles in the two epidermal cell types that are in direct contact with WCS417—trichoblasts that form root hairs and atrichoblasts that do not—implies a difference in potential for defense gene activation. While both cell types respond to WCS417, trichoblasts displayed both higher basal and WCS417-dependent activation of defense-related genes compared with atrichoblasts. This suggests that root hairs may activate root immunity, a hypothesis that is supported by differential immune responses in root hair mutants. Taken together, these results highlight the strength of cell-type-specific transcriptional profiling to uncover "masked" biological mechanisms underlying beneficial plant-microbe associations.

Key words: FACs, cell-type-specific transcriptomics, root immunity, beneficial rhizobacteria, suberin, root hair

Verbon E.H., Liberman L.M., Zhou J., Yin J., Pieterse C.M.J., Benfey P.N., Stringlis I.A., and de Jonge R. (2023). Cell-type-specific transcriptomics reveals that root hairs and endodermal barriers play important roles in beneficial plant-rhizobacterium interactions. Mol. Plant. **16**, 1160–1177.

INTRODUCTION

Plants are sessile organisms that cannot move in response to environmental changes. Instead, they adapt to changes by modifying the morphology and exudation of their roots or by activating a range of defense responses. The root system of the model plant *Arabidopsis thaliana* (*Arabidopsis*) consists of a primary root with branching lateral roots (Petricka et al., 2012; Motte et al., 2019).

Published by the Molecular Plant Shanghai Editorial Office in association with Cell Press, an imprint of Elsevier Inc., on behalf of CSPB and CEMPS, CAS.

Modifications in the spatial configuration of roots, the root system architecture, are especially important for water and nutrient uptake (Rogers and Benfey, 2015; Koevoets et al., 2016; Li et al., 2016; Shahzad and Amtmann, 2017). Root structure is also vital for adaptation to different conditions. Plant roots are organized in concentric cycles consisting of different cell types, with the outer cell types (trichoblasts, atrichoblasts) being in contact with the environment and the inner ones (cortex, endodermis, pericycle, vasculature) being indispensable for nutrient/water transport between below- and aboveground plant tissues (Wachsman et al., 2015; Stassen et al., 2021).

Exudation of specialized plant metabolites and structural fortification of inner cell types such as the endodermis are essential for nutrient uptake from the soil and a balanced interaction with the microbial communities surrounding the roots, known as the microbiome (Pascale et al., 2020; Kashyap et al., 2021). Exudates such as coumarins can facilitate iron uptake from the soil but also shape the root microbiome (Stringlis et al., 2018b; Harbort et al., 2020). Fortification of the endodermis includes the coating of endodermal cells by a hydrophobic polymer, suberin, and the deposition of lignin-based structures to form the Casparian strip in the junction between two adjacent endodermal cells (Naseer et al., 2012; Geldner, 2013; Barberon et al., 2016; Barberon, 2017). The amount of suberin deposition around endodermal cells is dynamically regulated during nutrient stresses and by the root microbiome (Barberon et al., 2016; Barberon, 2017; Salas-Gonzalez et al., 2021). An extra level of plant adaptation is achieved via the modification of root system architecture in response to beneficial soil microorganisms (Vacheron et al., 2013; Verbon and Liberman, 2016). In *Arabidopsis*, the number and/or length of lateral roots and root hairs increase in response to different rhizobacteria and fungi (Lopez-Bucio et al., 2007; Contreras-Cornejo et al., 2009; Zamioudis et al., 2013; Vacheron et al., 2018). All these chemical, morphological, or structural modifications of roots in response to the root microbiome rely on the prompt perception of microbes or their defense-eliciting molecules (microbe-associated molecular patterns [MAMPs]). These changes ultimately allow plants to maintain a beneficial interaction with their microbiome and avoid colonization by potentially harmful microbes (Millet et al., 2010; Beck et al., 2014; Wyrsch et al., 2015; Hacquard et al., 2017; Stringlis et al., 2018a; Teixeira et al., 2019; Colaianni et al., 2021).

Studies on the interaction between *Arabidopsis* and the beneficial rhizobacterium *Pseudomonas simiae* WCS417 (WCS417) unearthed different aspects of the interplay between plants and their associated beneficial microbes (Pieterse et al., 2021). WCS417 stimulates *Arabidopsis* growth (Zamioudis et al., 2013; Berendsen et al., 2015) and induces systemic resistance against many pathogens in *Arabidopsis* and several crop species (Pieterse et al., 1996, 2014). *Arabidopsis* responds to root colonization by WCS417 by inhibiting primary root growth and increasing the number of lateral roots and root hairs (Zamioudis et al., 2013; Stringlis et al., 2018a). The increased number of lateral roots upon WCS417 colonization is due to an increase in lateral root initiation events, observed as an increased number of lateral root primordia, and increased outgrowth of these primordia (Zamioudis et al., 2013). Lateral roots originate from pericycle cells, a cell layer surrounding the vasculature, and subsequently force their way through the endodermis, cortex, and finally the epidermis to protrude from the primary root (Malamy and Benfey, 1997; Moller et al., 2017; Otvos and Benkova, 2017; Du and Scheres, 2018). The plant hormone auxin is important for all phases of lateral root development (Du and Scheres, 2018). In line with this, the increase in lateral root number in response to WCS417 is dependent on auxin signaling (Zamioudis et al., 2013). Similarly, the WCS417-mediated increase in root hair number is dependent on auxin signaling (Zamioudis et al., 2013). In *Arabidopsis*, root hairs are formed by specialized cells in the epidermis: the trichoblasts. Trichoblasts and the atrichoblasts, another epidermal cell type, form the outermost root cell layer (Gilroy and Jones, 2000; Ryan et al., 2001; Vissenberg et al., 2020). The activity of several transcription factors, including TRANSPARENT TESTA GLABRA (TTG), CAPRICE (CPC), and WEREWOLF (WER), and the spatial localization of the cells, with cells located over two cortical cells becoming trichoblasts, regulate whether trichoblasts or atrichoblasts are formed (Vissenberg et al., 2020). In response to WCS417, the increased number of root hairs is due to an increased number of cortical cells and therefore an increased number of cells becoming trichoblasts (Zamioudis et al., 2013). A root system with a greater number of lateral roots and/or root hairs can mine more soil area for nutrients, has a larger surface to facilitate colonization by plant growth-promoting rhizobacteria (Lugtenberg and Kamilova, 2009; Vacheron et al., 2013), and has greater potential to release nutrient-mobilizing exudates (e.g., iron-chelating coumarins) (Robe et al., 2021).

Establishment and maintenance of beneficial plant-microbe interactions requires a fine balance between plant growth and defense. Beneficial microbes, such as pathogenic ones, can elicit MAMP-triggered immunity (MTI), which, when left unchecked, inhibits growth (Ma et al., 2021; Teixeira et al., 2021). Previous studies demonstrated that WCS417 can repress part of the root defense responses (Millet et al., 2010; Stringlis et al., 2018a), probably via the production of gluconic acid (Yu et al., 2019b). In recent years, many studies have demonstrated that the different cell types of the root can mount defense responses of varying levels depending on the MAMP and the responsible microbe colonizing the roots (Wyrsch et al., 2015; Rich-Griffin et al., 2020a; Zhou et al., 2020; Salas-Gonzalez et al., 2021). These studies suggest that, by compartmentalizing detection of microbes and activation of defense responses, the plant can maintain a proper growth-defense balance, avoiding costly and/or late defense activation (Yu et al., 2019a; Teixeira et al., 2019).

The structure of the *Arabidopsis* root system is defined by the distinct biological functions of each of its cell types. In parallel, specialized responses activated in each cell type upon microbial colonization allow plants to grow optimally in microbe-rich environments. Our previous studies on whole roots provided us with global information on the interaction between WCS417 and *Arabidopsis* (Verhagen et al., 2004; Zamioudis et al., 2014; Stringlis et al., 2018a). However, cell-type-specific transcriptomics can reveal which cell types respond to WCS417 most strongly or quickly, what responses are activated in each cell type, and how these responses contribute to successful colonization and subsequent effects on root

architecture and the establishment of a mutualistic interaction (Rich-Griffin et al., 2020b). Here, we used a set of fluorescent marker lines to isolate trichoblast, atrichoblast, cortical, endodermal, and vasculature cells with fluorescence-activated cell sorting (FACS) (Birnbaum et al., 2003, 2005; Brady et al., 2007a). To build a map of gene expression changes in the root, we transcriptionally profiled these cell populations after colonization by WCS417 in comparison with untreated control roots. Our data showed distinct cell-type-specific responses to WCS417 exposure. The most dramatic changes were seen in the cortex and endodermis, even though WCS417 strictly colonizes the root surface. In these inner cell layers, we observed an enrichment of genes associated with cell wall reorganization, reflecting the morphological observations of increased lateral root formation. We found evidence for functional specialization of the root epidermal cell types indicating a prominent role for root hair epidermal cells (trichoblasts) in activation of immunity upon bacterial colonization. Additionally, we found that endodermal cells increase their protective barrier in response to WCS417 by locally increasing suberin biosynthesis and deposition.

RESULTS

WCS417 rapidly induces root developmental changes

Plant growth-promoting rhizobacteria can affect plant root system architecture (Vacheron et al., 2013; Verbon and Liberman, 2016). In accordance with previous reports (Zamioudis et al., 2013; Stringlis et al., 2018a), WCS417 inhibited primary root length and increased the total number of lateral roots after 7 days of co-inoculation. After only 2 days of co-inoculation, we observed increased formation of lateral roots following bacteria application (Supplemental Figure 1). We reasoned that, by studying this time point using cell-type-specific transcriptomics, we would capture the transcriptional events in different cell types underlying early plant modifications in response to the epiphytic bacterium WCS417 and identify processes involved in the establishment of a beneficial plant-microbe interaction.

Cell-type-specific transcriptional profiling of the *Arabidopsis* root

To create a spatial map of root transcriptional changes in response to colonization by WCS417, we isolated several root cell types using FACS. First, we confirmed that WCS417 does not affect the expression pattern of *GREEN FLUORESCENT PROTEIN* (*GFP*) when driven by the cell-type-specific promoters *WEREWOLF* (*WER*; atrichoblast), *COBRA-LIKE 9* (*COBL9*; trichoblast), *315* (cortex), *SCARECROW* (*SCR*; endodermis), or truncated *WOODENLEG* (*WOL*; vasculature) (Figure 1A). Subsequently, we grew the transgenic lines carrying these promoter-GFP fusions under high-density conditions and exposed them to WCS417 in addition to control treatment. Two days after inoculation, we harvested the roots, performed FACS, and isolated RNA (Figure 1B).

To determine the success of the sorting procedure, we checked the expression of the marker genes *WER*, *COBL9*, *315*, *SCR*, and *WOL* in our transcriptomic dataset (Figure 2A). The expression of each of these markers should be highest in the FACS samples obtained from the transgenic plant lines in which the corresponding promoter was used to drive *GFP* expression. Indeed, the expression of *WER*, *COBL9*, *315*, and *SCR* is highest in the samples obtained from their respective lines (Figure 2B). The expression of *WOL* is not enriched in the vasculature line, but we did observe enrichment for the well-established vasculature marker genes, *INCURVATA4*, *SHORTROOT* (*SHR*), and *ZWILLE* (*ZLL*) (Figure 2C), suggesting the successful enrichment of vasculature cells. Notably, this line uses a truncated *WOL* promoter to drive GFP expression (Mahonen et al., 2000) rather than the full promoter, indicating that only the truncated *WOL* promoter is in fact vasculature cell type specific. By analyzing the expression of *WOL* and these three vasculature marker genes in the recently published single-cell root atlas by Shahan et al. (2022), we could confirm this observation (Supplemental Figure 2). Notably, *WOL* expression appears in all cells and cell types, whereas the expression of *INCURVATA4*, *SHR*, and *ZLL* is restricted to the xylem, phloem, pericycle, and procambium cell types (Supplemental Figure 2B). Similar to our findings shown in Figure 2C, *SHR* is an exception as it has been found also in endodermal cells. To further evaluate whether the cell-type-specific identities were preserved in the experiment and during the sorting procedure, we compared the expression of the top 50 cell-type-specific marker genes from the single-cell root atlas for each relevant cell type (Shahan et al., 2022). This analysis corroborated the appropriate identities for the different cell types (i.e., cell-type-specific marker genes are expressed highest in FACS samples obtained from the same cell type) and shows that the cellular identities of WCS417-treated cells (WCS) appear similar to the untreated, control ones (NB) (Supplemental Figure 3A). Interestingly, atrichoblast cells that are sorted using the *WEREWOLF* (*WER*) *proWER*::*GFP* selective marker appear enriched for lateral root cap, atrichoblast, and to some extent trichoblast marker gene expression. Finally, we compared the mean gene expression level of all detected genes in sorted versus unsorted cells, with and without treatment. These gene expression profiles are highly correlated (R^2 = 0.88 and 0.89 for control [NB] and WCS417-treated roots, respectively), indicating that the sorting procedure itself did not have a major effect on the global gene expression landscape (Supplemental Figure 3B).

To study the global similarities and dissimilarities among samples and treatments, we performed multidimensional scaling on gene expression levels. The transcriptional profiles cluster primarily by sample type ($P_{sample\ type}$ = 0.001; Figure 2D). The cortical and endodermal cells cluster close together, as do the two epidermal cell types. This is in line with the known development of the *Arabidopsis* root, in which the cortex and endodermis develop from a shared stem cell population, as do the trichoblasts and atrichoblasts (Dolan et al., 1993; Van den Berg et al., 1995; Shahan et al., 2022), and fits with the Uniform Manifold Approximation and Projection for Dimension Reduction projection of the single-cell root atlas by Shahan et al. (2022) (Supplemental Figure 2A). In addition to the sample-type effect, we find an effect of bacterial treatment on gene expression ($P_{treatment}$ = 0.005; Figure 2D). When comparing gene expression patterns of samples within sample types, each cell type except the vasculature clusters primarily based on bacterial treatment (Figure 2E).

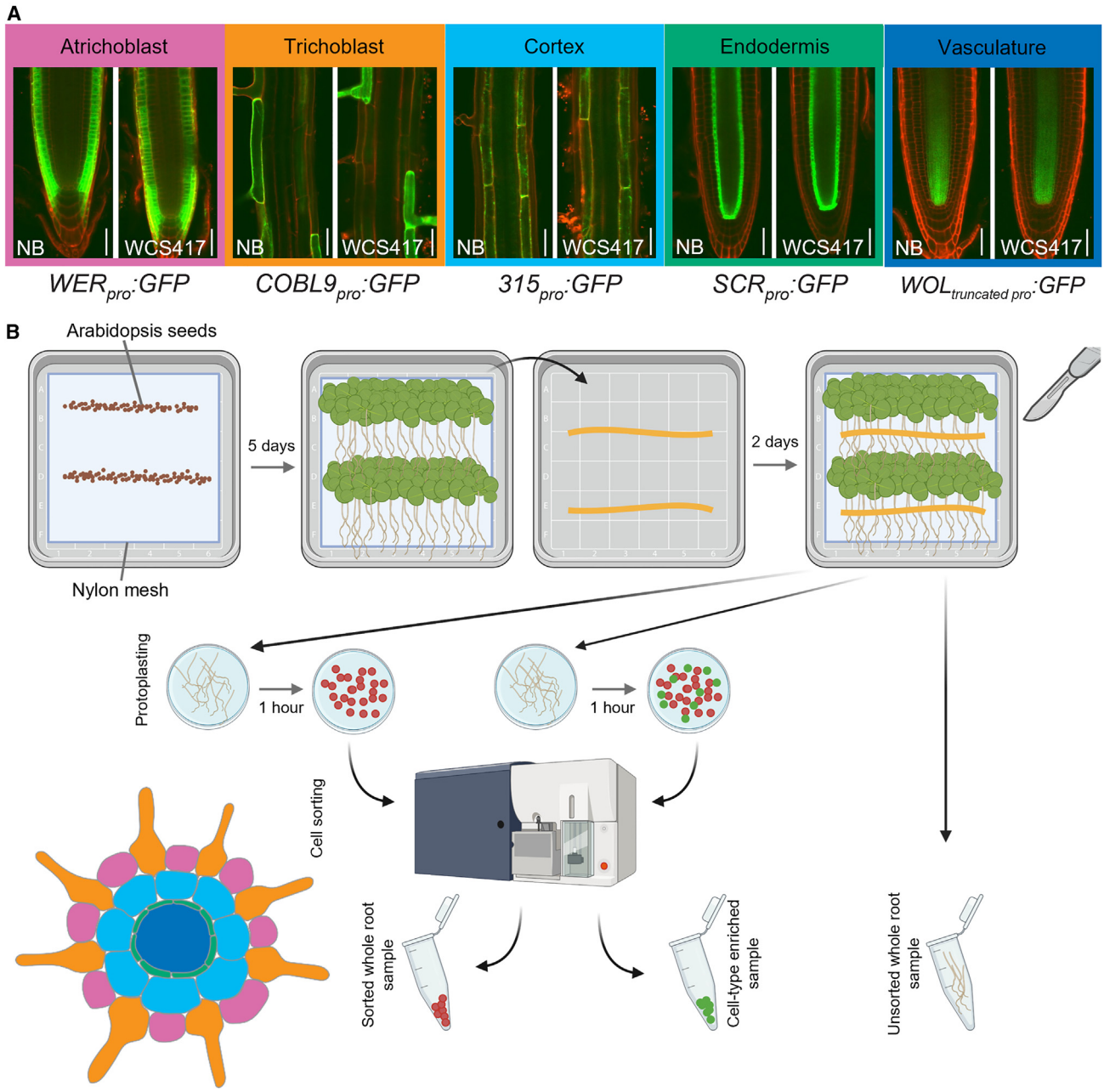

Figure 1. Exposure of five transgenic plant lines to WCS417 to obtain cell-type-specific samples by performing FACS.

(A) Sterile and WCS417-exposed plants from the transgenic plant lines *WEREWOLF*$_{pro}$*:GFP* (*WER*, immature epidermis and atrichoblast), *COBRA-LIKE9*$_{pro}$*:GFP* (*COBL9*, trichoblast), *315*$_{pro}$*:GFP* (*315*, cortex), *SCARECROW*$_{pro}$*:GFP* (*SCR*, endodermis), and *WOODENLEG*$_{truncated\_pro}$*:GFP* (*WOL*, vasculature). Pictures of the seedlings were taken all along the root from day five (day of bacterial inoculation) until day seven. GFP settings were kept the same between bacteria-exposed and sterile-grown plants. Representative images are shown, and colored text boxes are used to match with the coloring of cell types in the *Arabidopsis* root cross section graphic (bottom left of figure).

(B) Experimental design used to obtain WCS417-treated and control samples enriched for one out of five root cell types. Sterilized and vernalized *Arabidopsis* seeds were sown on 1× MS 1% sucrose plates and left to grow in long-day conditions. Five days later, half of the plants of each line were transferred on their mesh onto 1× MS 1% sucrose plates with WCS417. Plants were left to grow for a further 2 days of growth before root harvest. Wild-type Col-0 roots were either directly flash-frozen (unsorted control) or protoplasted and put through the cell sorter, collecting non-fluorescent cells (sorted control). Transgenic lines with cell-type-specific *GFP* expression were similarly protoplasted and put through the cell sorter for FACS.

Next, we determined which genes are differentially expressed (differentially expressed genes [DEGs]) in response to WCS417 in each of the cell types compared with untreated roots (Supplemental Tables 1A–1C). The number of DEGs differs greatly among the cell types, ranging from 30 in the vasculature to 1109 in the cortex (Figure 3A). Interestingly, the cortical and endodermal cells, which do not interact directly with the strictly epiphytic WCS417 bacterium, displayed the largest number of

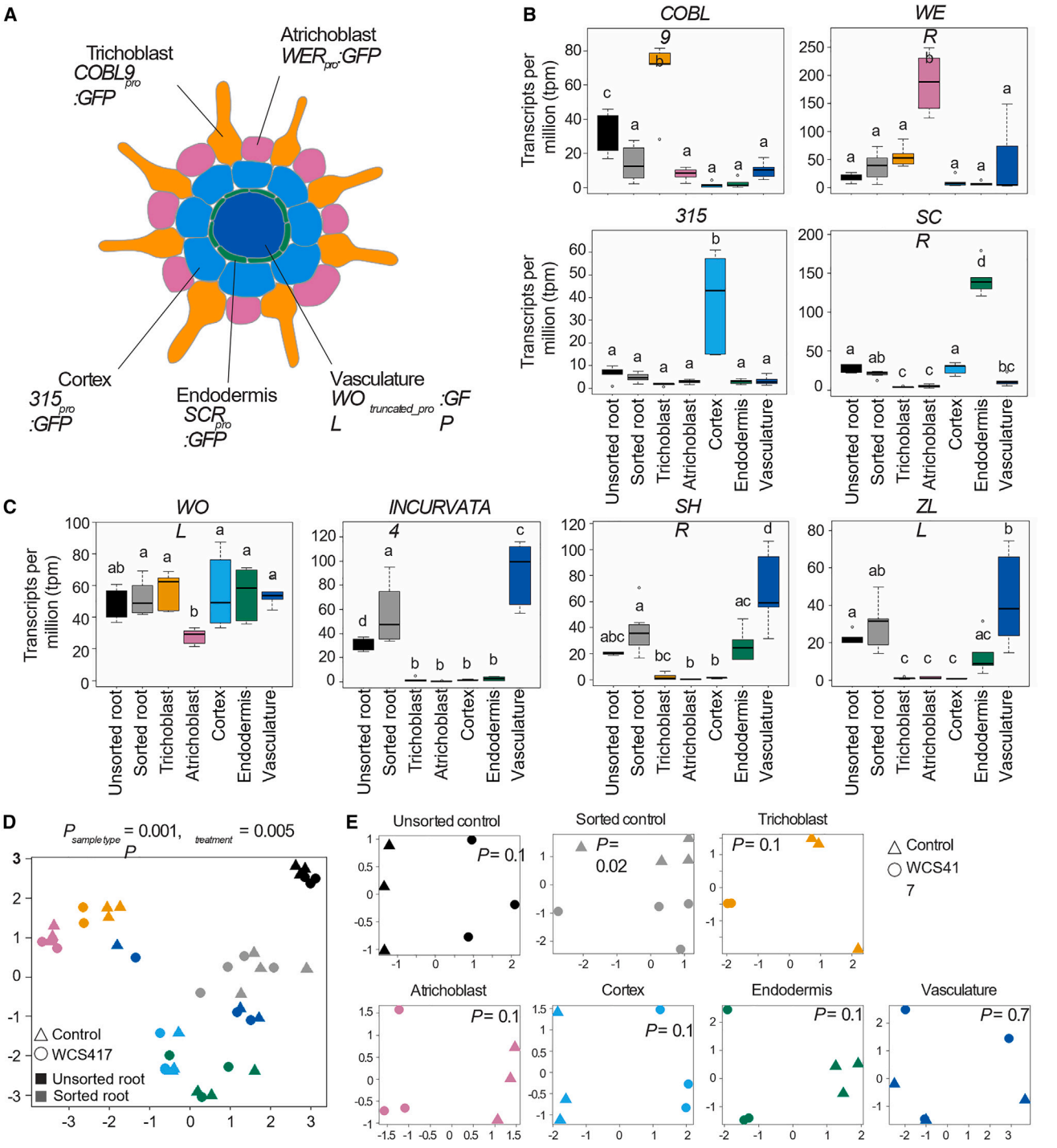

Figure 2. Gene expression differences among the samples reflect *Arabidopsis* root development patterns.

(A) Schematic cross section of the *Arabidopsis* root, with each cell type labeled with the *promoter::GFP* fusion that was used to enrich samples for that cell type by FACS.

(B) mRNA levels of the marker genes *COBL9*, *WER*, *315*, and *SCR*.

(C) mRNA levels of the marker gene *WOL*, and of the vasculature-specific genes *INCURVATA4*, *SHR*, and *ZLL*. Data were analyzed with an ANOVA test followed by the Tukey *post hoc* test in R ($p < 0.05$). GFP, green fluorescent protein; COBL9, COBRA-LIKE 9; WER, WEREWOLF; SCR, SCARECROW; WOL, WOODENLEG; SHR, SHORTROOT; ZLL, ZWILLE.

(D and E) Multidimensional scaling (MDS) plot of counts (log scale) per million of all samples **(D)** and per cell type **(E)**. WCS417-exposed samples are represented by circles and control, untreated samples by triangles. Colors in **(B)–(E)** correspond to the color scheme of the schematic in **(A)**. Black samples represent the unsorted wild-type roots, grey represents the sorted wild-type roots. In **(E)**, "*P*" represents the p value of the WCS417-treatment effect.

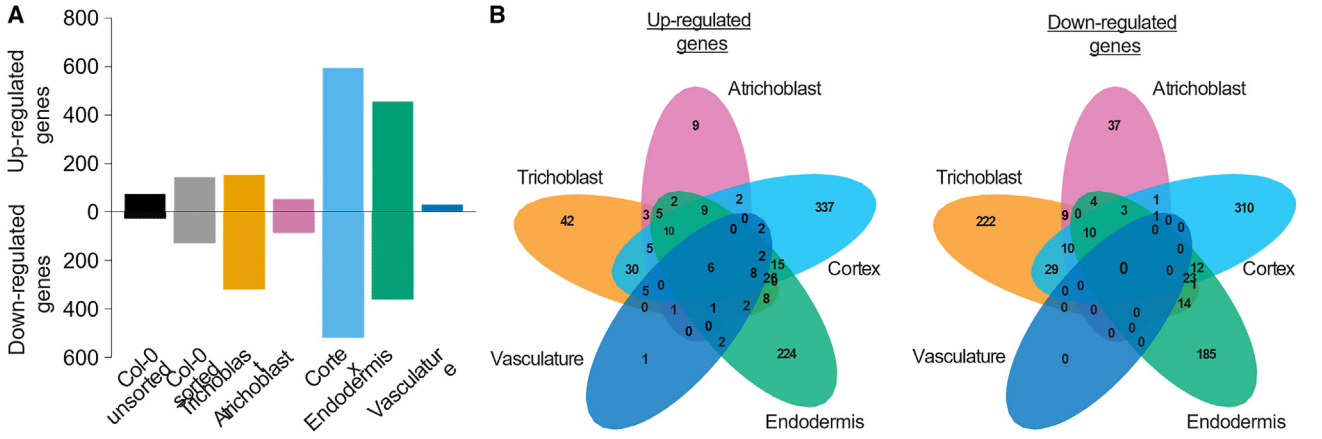

Figure 3. Types of root cells show unique responses to root colonization by WCS417.
(A) Number of DEGs upon WCS417 application found in the respective samples (false discovery rate [FDR] <0.1; −2 < log2FC > 2).
(B) Venn diagrams showing the overlap in genes affected by WCS417 treatment in the five studied cell types.

DEGs (1109 and 815, respectively), while the trichoblast and atrichoblast cells, which are in direct contact with WCS417, displayed far fewer DEGs (469 and 137, respectively). Apart from a quantitative difference, the response is also qualitatively different between cell types: of the 1862 DEGs across all five cell types, 72% are affected in only one cell type and only six genes are affected in all cell types (Figure 3B). Notably, the majority of genes affected in only a single cell type are not identified as differentially expressed in the whole root, while most genes affected in four or five cell types are identified as either up- or downregulated in whole roots (Supplemental Table 2). In contrast, the majority of genes found to be up- or downregulated in the sorted or unsorted control were identified as differentially expressed in response to WCS417 in one or more cell types (Supplemental Table 3). In conclusion, genes affected in only single cell types were often not identified as differentially expressed in the whole root. This explained the higher number of identified DEGs in the cell-type-specific dataset compared with the sorted whole root (1862 genes versus 270 genes; Figure 3A).

Higher responsiveness of trichoblasts to WCS417 as compared with atrichoblasts

To identify the biological processes affected by WCS417 colonization in the different cell types, we conducted biological process Gene Ontology (GO) term enrichment analyses on the DEGs (Supplemental Tables 4–13). Most significant among the upregulated DEGs in the trichoblasts, cortex, endodermis, and vasculature are processes related to defense and immunity (Supplemental Table 4). Interestingly, defense activation is not prominent in atrichoblasts in response to WCS417 (Supplemental Table 6). This suggests that the two cell types directly in contact with WCS417 activate distinct biological processes, as could be expected from the limited overlap in DEGs between these cell types (Figures 3B and 4A). To further analyze these differences, we examined the expression of the genes within the GO term defense response (GO: 0006952) that are differentially upregulated in one or both epidermal cell types. We identified 37 such genes in total, 28 specifically for trichoblast cells, one for atrichoblasts, and eight were found differentially upregulated in both epidermal cell types (Supplemental Table 14). Notably, most of these genes appear elevated in both WSC417-treated (WCS) epidermal cell types upon comparison of their normalized expression levels (Figure 4B), but the overall relative increase in trichoblast cells is more pronounced following WCS417 inoculation (Figures 4C and 4E). To further assess the relative importance of trichoblast over atrichoblast cells with regard to the defense response, we next examined the normalized expression of all defense response-related genes (GO: 0006952) in both cell types, irrespective of differential expression. This analysis confirmed that these genes are expressed at higher levels in trichoblast cells (Figure 4D), but it also indicates that only a part of the defense-related genes respond to WCS417 application as the treatment effect is now largely absent.

Root hairs contribute to microbial perception and affect plant responses to WCS417

We found that, upon exposure to WCS417, trichoblasts, in particular, appear to activate defense-related genes, illustrated by the enrichment for defense gene expression in these cells (Figures 4B and 4C; Supplemental Table 4). This could indicate that cell types destined for the formation of root hairs (trichoblasts) might be more sensitive to microbial signals and this sensitivity could affect plant responses to microbes. To test this hypothesis, we assessed the effect of WCS417 on two mutants with contrasting patterns of root hair formation: *cpc*, which forms fewer root hairs compared with wild-type, and *ttg1*, where most epidermal cells produce root hairs. We grew *Arabidopsis* wild-type Col-0 plants and the two mutants in plates containing 10^5 colony-forming units (CFU). ml^{-1} WCS417 based on a protocol developed by Paredes et al. (2018) and measured growth-promotion traits and levels of root colonization. Interestingly, the beneficial effects of WCS417 were less pronounced on both mutants compared with wild-type plants, since relative changes in fresh shoot weight, primary root length, and number of lateral roots were significantly lower (Figures 5A–5C; Supplemental Figure 4). Nevertheless, WCS417 colonization was comparable between wild-type and mutant roots (Figure 5D). We then reasoned that the number of root hairs might also affect defense responses to WCS417 and the bacterial MAMP flg22. For this, we tested the expression of

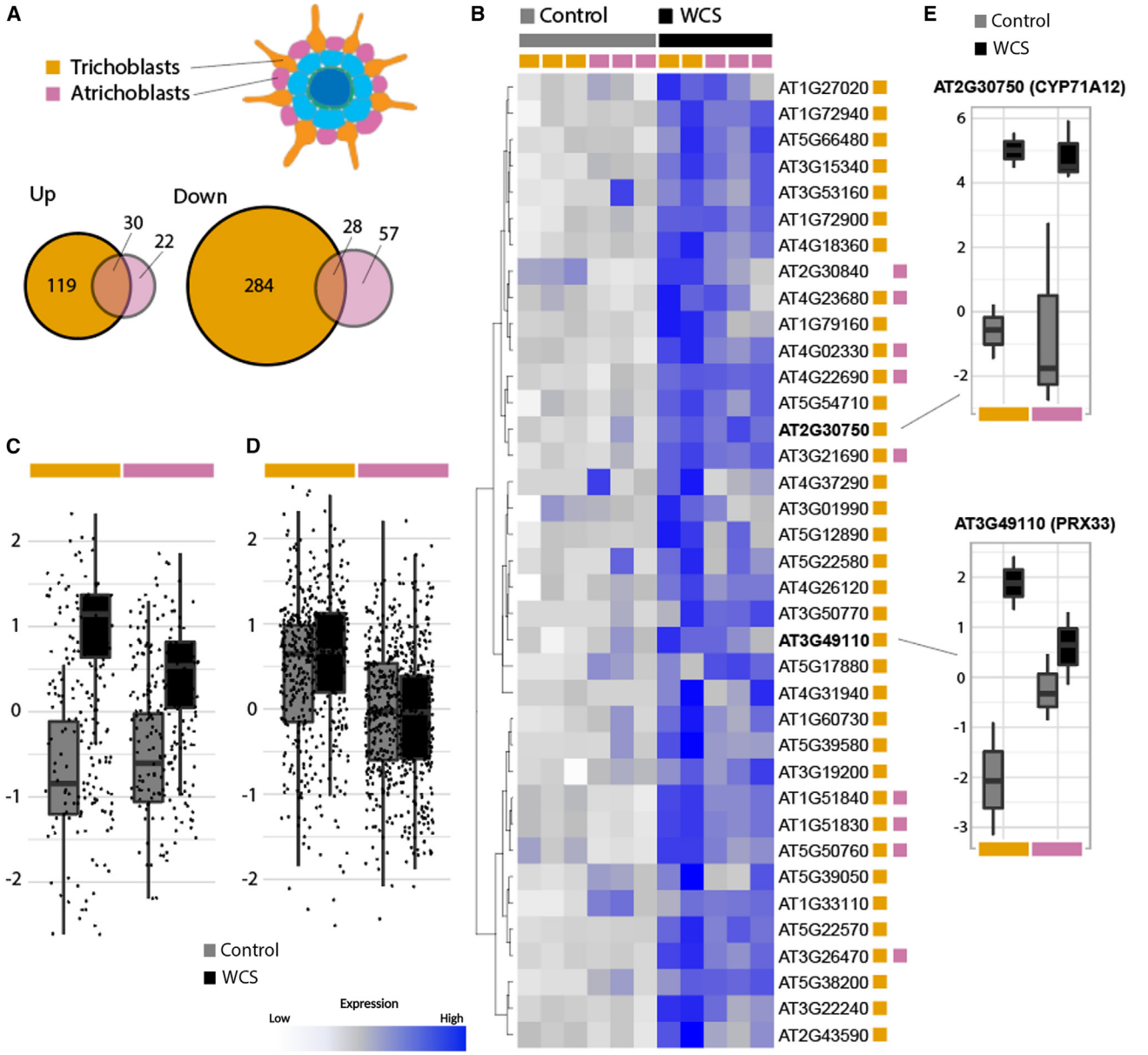

Figure 4. High responsiveness of trichoblasts to root colonization by WCS417.

(A) Overlap of the DEGs in response to WCS417 in the trichoblasts and atrichoblasts.

(B) Heatmap of the expression of genes associated with the GO term defense response (GO: 0006952) that were differentially expressed (DE) in either or both epidermal cell types in response to WCS417. DE status in either cell type shown by the colored squares (trichoblasts, orange; atrichoblasts, pink). Heatmap is scaled by row and gene expression is shown as the normalized log counts per million, with low gene expression in white and high expression in dark blue.

(C) Scaled (per-gene) expression levels of DEGs as shown in **(B)**.

(D) Scaled (per-gene) expression levels of all genes associated with GO: 0006952.

(E) Expression of candidate marker genes *CYP71A12* and *PRX33* as normalized log counts per million.

WCS417- and flg22-responsive MTI-related genes *MYB51* (MYB DOMAIN PROTEIN 51; *AT1G18570*), *CYP71A12* (CYTOCHROME P450, FAMILY 71, SUBFAMILY A, POLYPEPTIDE 12; *AT2G30750*), *PRX33* (PEROXIDASE 33; *AT3G49110*), and *LECRK-IX.2* (L-TYPE LECTIN RECEPTOR KINASE IX.2; *AT5G65600*) (Millet et al., 2010; Stringlis et al., 2018a). MYB51 and CYP71A12 have roles in indole glucosinolate and camalexin biosynthesis respectively (Millet et al., 2010), PRX33 is a cell wall peroxidase involved in the generation of reactive oxygen species during defense activation (Kaman-Toth et al., 2019), and LECRK-IX.2 is an L-type lectin receptor kinase that acts as a positive regulator of MTI (Luo et al., 2017). We previously found that all four of these genes are induced in young Col-0 seedlings at multiple, consecutive time points by both WCS417 and flg22 treatment. In the current dataset, we found that all four genes are induced in one or more cell types, with the exception of *LECRK-IX.2*. Specifically, *CYP71A12* and *PRX33* are induced in trichoblast and cortical cells, and in endodermal cells in the

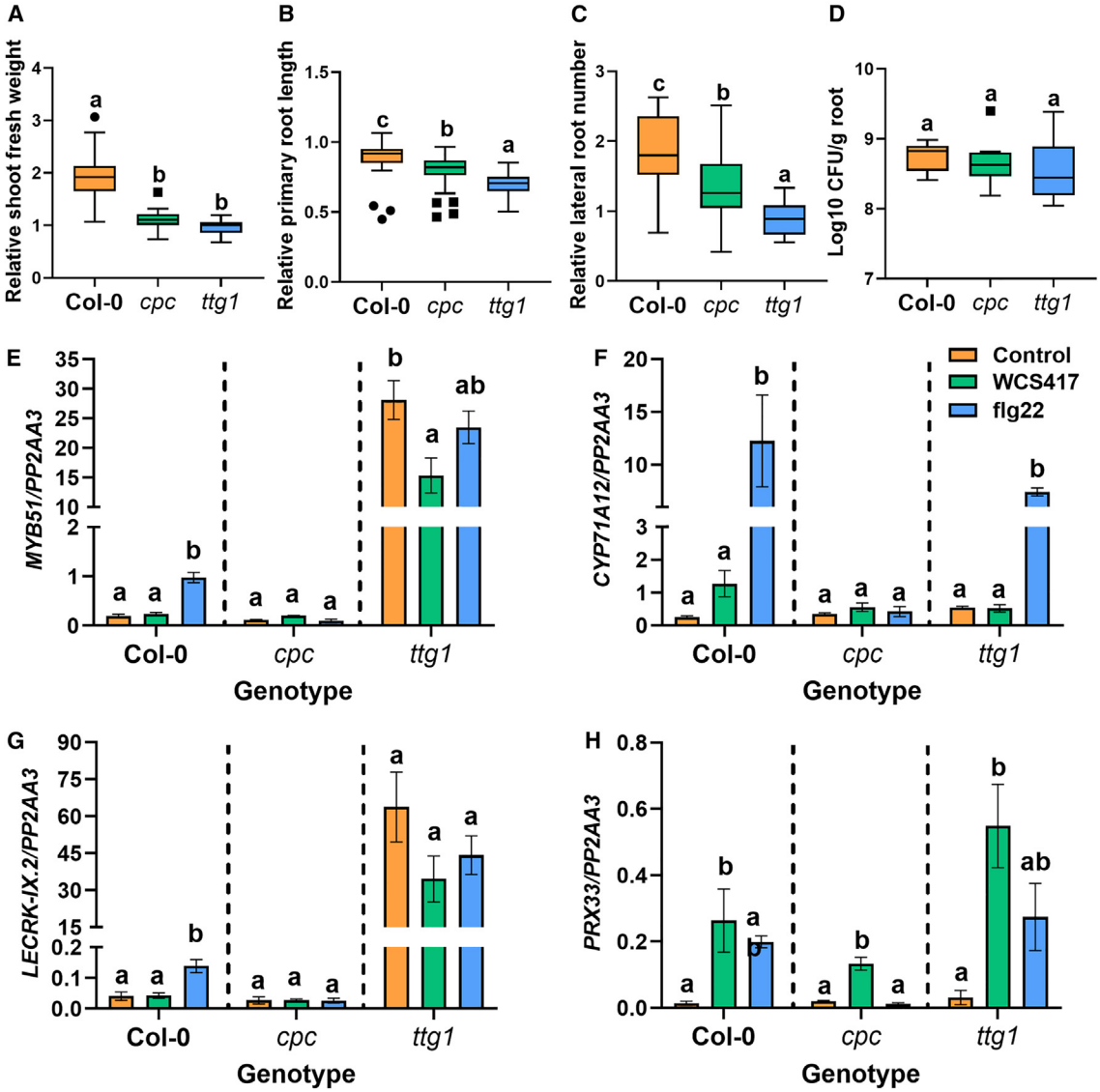

Figure 5. *Arabidopsis* root hair mutants display differential responses to WCS417.

(A–D) Relative **(A)** shoot fresh weight, **(B)** primary root length, **(C)** lateral root number, and **(D)** colonization levels of WCS417 on roots of Col-0, *cpc*, and *ttg1* genotypes at 7 days after seedlings were transferred to plates with Hoagland medium (0% sucrose) containing 10^5 CFU ml^{-1} WCS417. Different letters indicate statistically significant differences across genotypes (one-way ANOVA, Tukey's test; $p < 0.05$). In the case of growth parameters, $n = 39–40$, and in root colonization, $n = 8$. Relative values were calculated by dividing the value of a parameter in each WCS417-inoculated seedling by the average value of all the mock seedlings.

(E–H) Relative expression levels of **(E)** *MYB51*, **(F)** *CYP71A12*, **(G)** *LECRK-IX.2*, and **(H)** *PRX33* as quantified by qRT-PCR. The reference gene *PP2AA3* (*AT1G13320*) was used for normalization. Expression was evaluated in roots of 8-day-old seedlings at 6 h after inoculation with WCS417 (OD_{600} equal to 0.1, 10^8 CFU ml^{-1}) or treated with 1 μM flg22. Error bars represent SEM. Different letters represent statistically significant differences among control, WCS417, and flg22 in same plant genotype as indicated by the dashed separating lines (one-way ANOVA, Tukey's test; $p < 0.05$, $n = 3–4$).

case of *CYP71A12*, while *MYB51* is induced in endodermal cells only. WCS417- and flg22-induced expression patterns of *MYB51* (Figure 5E), *CYP71A12* (Figure 5F), *LECRK-IX.2* (Figure 5G), and *PRX33* (Figure 5H) are affected in mutants with altered root hair density, in which mutant *cpc* displayed a reduced response to the elicitors, while *ttg1* appeared unresponsive to elicitation but displayed generally elevated expression of *MYB51* and *LECRK-IX2*. Overall, we found that the presence of root hairs affects the expression of MTI-related genes, and the beneficial effects by WCS417 in mutants with altered root hair density were less pronounced.

WCS417 might facilitate lateral root formation by loosening cell walls of cell layers overlaying lateral root primordia

Among the downregulated DEGs in the cortical and endodermal cell layers upon WCS417 treatment, we observed many genes related to processes associated with root and tissue development and cell-wall organization or biogenesis. Conversely, cell wall modification (GO: 0042545) was enriched among the upregulated DEGs in the endodermis (Supplemental Tables 9– 12). Cell wall remodeling and cell volume loss in the cortex and endodermis

are known to be required to accommodate emerging lateral roots and are possibly even required for the initiation of lateral root primordia (Vermeer et al., 2014; Stoeckle et al., 2018). Many of the processes enriched within the downregulated genes in the cortex are related and are typically relatively aspecific. However, when considering the odds ratio of observations, we noted xylan metabolism (GO: 0045491) as one of the more specific biological processes significantly overrepresented in the downregulated genes. Upon inspection of the genes within this process, we observed significant downregulation of several genes, i.e., *GUX2* (GLUCURONIC ACID SUBSTITUTION OF XYLAN 2; *AT4G33330*), *IRX9* (IRREGULAR XYLEM 9; *AT2G37090*), and *IRX14-L* (IRREGULAR XYLEM 14-LIKE; *AT5G67230*), involved in glucuronoxylan biosynthesis (GO: 0045491). To characterize the genes related to this process in more detail we plotted the expression of all genes within this process across all cell types (Supplemental Figure 5A). Although only three out of the 12 genes annotated in this process in *Arabidopsis* were significantly downregulated, many of the other genes were in fact also repressed upon bacterial treatment. Overall we observed the highest expression of these genes in vasculature cells, while they were particularly repressed in the cortical and endodermal cells (Supplemental Figure 5B). Among the genes upregulated in the endodermis with involvement in cell wall modification were genes that encode polygalacturonases, which have been shown to be expressed at the site of lateral root emergence. They have been implicated in cell separation, possibly to accommodate emerging lateral roots (Ogawa et al., 2009). Upregulation of these and other genes involved in cell wall modification and downregulation of genes involved in cell wall biogenesis, particularly xylan biosynthesis, in the cortex and endodermis might therefore be an integral part of the molecular and physiological changes that take place in response to WCS417, which lead to the observed increase in the number of lateral roots (Supplemental Figure 1; Zamioudis et al., 2013). To investigate the predicted effect of cell wall loosening, we obtained mutants for selected genes, *IRX9*, *IRX9L* (IRREGULAR XYLEM 9-LIKE; *AT1G27600*), *IRX14* (IRREGULAR XYLEM 14; *AT4G35890*), and *IRX14L*, that are repressed by WCS417 and involved in glucuronoxylan metabolism (Supplemental Figure 5A). All four genes are involved with xylan synthesis and backbone elongation, and, accordingly, mutants display irregular xylem (IRX) phenotypes (Wu et al., 2010). We assessed growth promotion, colonization, and lateral root emergence on all *IRX* mutants in comparison with wild-type Col-0 plants. All mutants displayed similar promotion of plant shoot biomass to Col-0 following WCS417 inoculation (Supplemental Figure 6A), and WCS417 population density was comparable between Col-0 and mutant plants (Supplemental Figure 6B). Interestingly, upon WCS417 colonization, three out of the four tested mutants, i.e., *irx14*, *irx14-L*, and *irx9-L*, developed significantly more lateral roots per centimeter of primary root compared with Col-0 (+41%–78%; $p < 0.01$). These observations are consistent with our hypothesis that bacterial colonization leads to a repression of cell wall fortification supporting accelerated emergence of lateral root primordia.

WCS417 induces suberin biosynthesis in endodermal cells

Defense in general is the most significant process affected in our cell-type-specific gene expression analysis. This is, in part, because many genes are known to be part of this GO term. To study biological processes in which fewer genes are involved, such as the xylan metabolism mentioned earlier, we subsequently studied enriched GO terms with the highest odds ratios (i.e., with the largest difference in expected versus actual counts). In this analysis, we found a significant enrichment for suberin biosynthesis (GO: 0010345) in the endodermis, specifically, with an odds ratio of 20.9 (Supplemental Table 10). Suberin is a hydrophobic polymer deposited between the primary cell wall and the plasma membrane of endodermal cells. There, suberin, together with the lignin-containing Casparian strip that builds tight junctions between adjacent endodermal cells, blocks free movement of water and nutrients into the endodermis and consequently the innermost cell layers of the *Arabidopsis* root (Geldner, 2013; Barberon, 2017). Like the formation of lateral roots and root hairs, the production of suberin is affected by nutrient availability (Barberon et al., 2016). In addition, recent data suggest that suberin and the Casparian strip are involved in the interaction between plants and root-associated commensals and soil-borne phytopathogens (Froschel et al., 2020; Salas-Gonzalez et al., 2021).

We analyzed the effect of WCS417 on genes related to suberin production, such as MYB transcription factors *MYB9* (*AT5G16770*), *MYB36* (*AT5G57620*), *MYB41* (*AT4G28110*), *MYB53* (*AT5G65230*), *MYB92* (*AT5G10280*), *MYB93* (*AT1G34670*), and *MYB107* (*AT3G02940*) suggested to activate suberin biosynthesis (Kosma et al., 2014; Lashbrooke et al., 2016; Shukla et al., 2021), and enzymes involved in suberin biosynthesis, including β-KETOACYL-CoA-SYNTHASEs *KCS2* (*AT1G04220*) and *KCS20* (*AT5G43760*), fatty acid cytochrome P450 oxidases *CYP86A1* (*AT5G58860*) and *CYP86B1* (*AT5G23190*), FATTY ACUL-CoA REDUCTASEs *FAR1* (*AT5G22500*), *FAR4* (*AT3G44540*) and *FAR5* (*AT3G44550*), GLYCEROL-3-PHOSPHATE SN2-ACYLTRANSFERASEs *GPAT5* (*AT3911430*), and *GPAT7* (*AT5G06090*) as well as transporters such as the ATP-binding cassette transporter proteins *ABCG1* (*AT2G39350*), *ABCG2* (*AT2G37360*), *ABCG6* (*AT5G13580*), *ABCG11* (*AT1G17840*), *ABCG16* (*AT3G55090*), and *ABCG20* (*AT3G53510*) (Panikashvili et al., 2010; Yadav et al., 2014; Vishwanath et al., 2015; Barberon, 2017). As expected, based on the available literature and our GO term analyses, spatial gene expression patterns showed that suberin biosynthesis is primarily restricted to the endodermis and is significantly induced by WCS417 (Figures 6A and 6B). Next, we assessed biosynthesis and deposition of suberin following bacterial colonization by staining roots with Fluorol Yellow (FY) to visualize suberin (Barberon et al., 2016). We found that WCS417 colonization indeed led to an increase of suberin in the endodermis as quantified by a decreased distance from the root tip to the continuously suberized root zone (Figures 6C and 6D).

Root endodermal barriers have a role in colonization by WCS417 and the subsequent activation of defense responses

Based on the increased suberization following colonization by WCS417 (Figure 6), we hypothesized that endodermal barriers might play a role in the interaction between *Arabidopsis* and WCS417. To test this, we grew wild-type plants and *myb36-2*/*sgn3-3* mutants with developmentally delayed and reduced endodermal barriers (Salas-Gonzalez et al., 2021) and

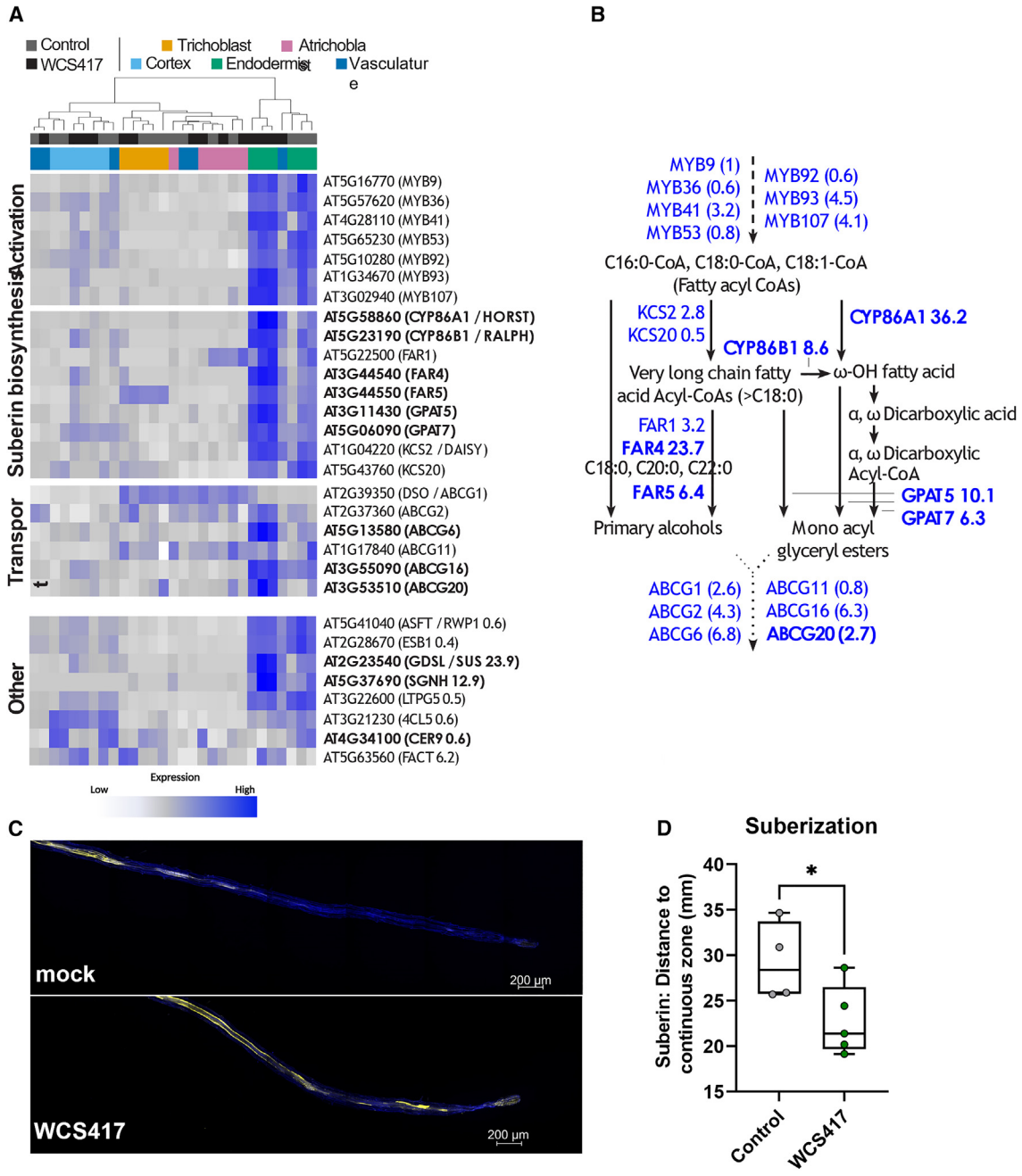

Figure 6. WCS417 induces suberization of the endodermis.

(A) Heatmap of the expression of genes known to be involved in suberin biosynthesis (GO: 0010345, suberin biosynthetic process; Lashbrooke et al., 2016; Vishwanath et al., 2015). Heatmap is scaled per row (gene). Genes that are significantly upregulated (logFC > 2, FDR < 0.1) by WCS417 in the endodermis are shown in bold.

(B) Overview of the suberin biosynthesis pathway, its activation, and suberin monomer transport out of the cell, adapted from Vishwanath et al., (2015). Genes known to be involved in these processes are shown in blue, and fold changes as found in our dataset in response to WCS417 are shown. Statistical significantly DEGs (FDR < 0.1) are depicted in bold. Dashed lines show activation, solid lines show compound conversions, dotted lines show transport processes.

(C and D) Suberization in roots of 7-day-old *Arabidopsis* at 2 days after they were transferred in Hoagland plates containing WCS417. Suberin was visualized using FY staining and quantified as the distance from the root tip to the continuous zone of suberization in roots of *Arabidopsis* (n = 4–5). Representative confocal images are shown.

performed experiments with WCS417 similar to those described above for root hair and cell wall assembly mutants. The effects of WCS417 on wild-type and endodermal barrier mutant plants were similar in terms of shoot growth promotion (Figure 7A; Supplemental Figure 7A). This was not the case for primary root length and lateral root formation, with WCS417 having a more

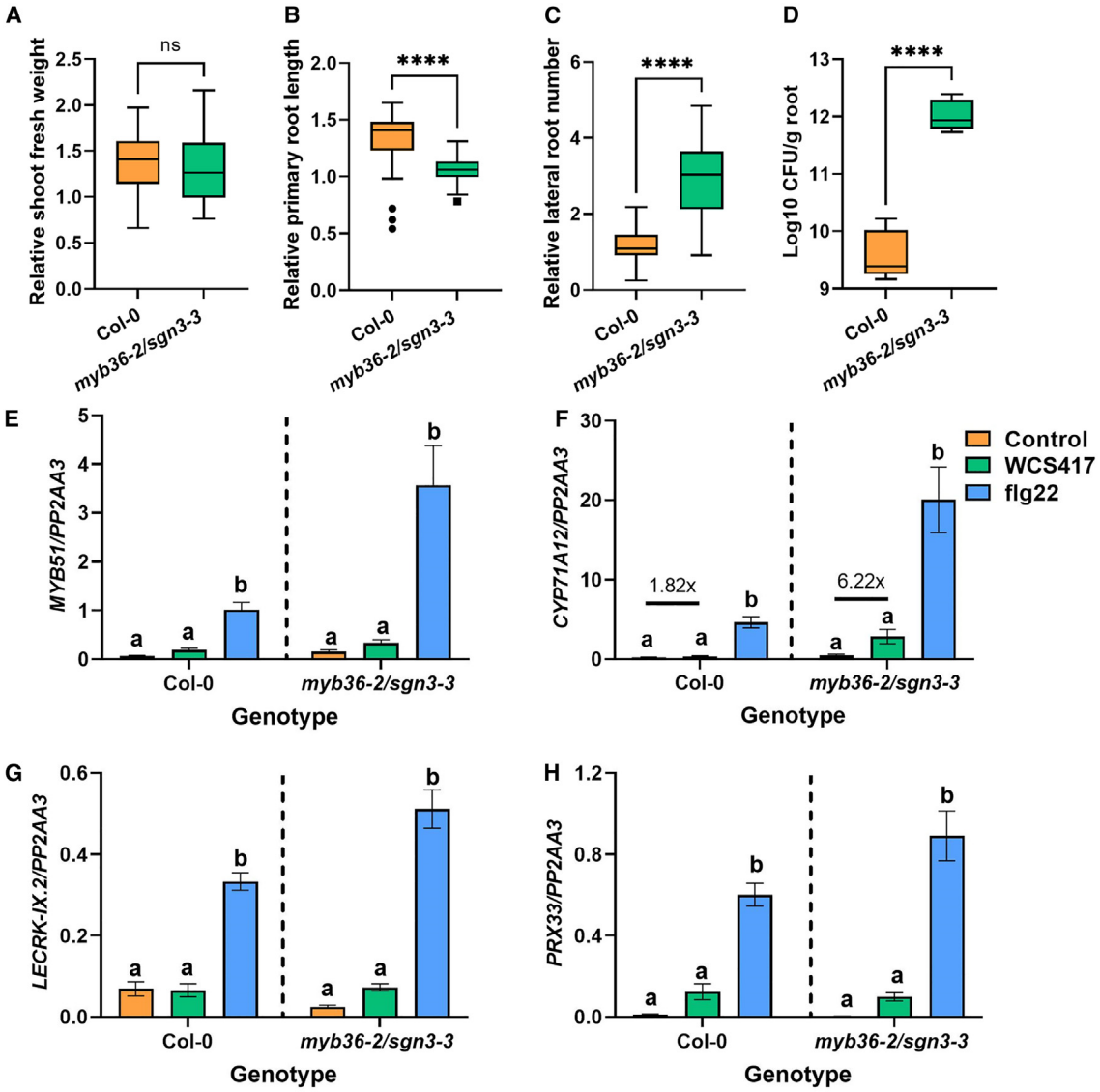

Figure 7. Root endodermal barrier integrity is needed for balanced interaction with WCS417.

(A–D) Relative **(A)** shoot fresh weight, **(B)** primary root length, **(C)** lateral root number, and **(D)** colonization levels of WCS417 on roots of Col-0 and *myb36-2/sgn3-3* at 7 days after seedlings were transferred to plates with Hoagland medium (0% sucrose) containing 10^5 CFU ml^{-1} WCS417. Asterisks indicate significant differences between genotypes following WCS417 inoculation (Student's *t*-test; $^*p < 0.05$, $^{**}p < 0.01$, $^{***}p < 0.001$,$^{****}p < 0.0001$; ns, not significant). In the case of growth parameters, $n = 30$, and in root colonization, $n = 6$. Relative values were calculated by dividing the value of a parameter in each WCS417-inoculated seedling by the average value of all the mock seedlings.

(E–H) Relative expression levels of **(E)** *MYB51*, **(F)** *CYP71A12*, **(G)** *LECRK-IX.2*, and **(H)** *PRX33* as quantified by qRT-PCR. The reference gene *PP2AA3* (*AT1G13320*) was used for normalization. Expression was evaluated in roots of 8-day-old seedlings at 6 h after inoculation with WCS417 ($OD_{600} = 0.1$, 10^8 CFU ml^{-1}) or treated with 1 μM flg22. Error bars represent SEM. Different letters represent statistically significant differences among control, WCS417, and flg22 in same plant genotype as indicated by the dashed separating lines (one-way ANOVA, Tukey's test; $p < 0.05$, $n = 3$–4).

pronounced effect on *myb36-2/sgn3-3* plants compared with wild-type plants (Figures 7B and 7C; Supplemental Figures 7B and 7C). Next, we assessed the colonization levels of WCS417 on roots of wild-type and mutant plants. Remarkably, WCS417 colonization levels were much higher (almost 100 times) on *myb36-2/sgn3-3* roots compared with the wild-type (Figure 7D), indicating that disruption of endodermal barriers greatly affected the interaction with WCS417. To further confirm this observation, we studied the expression of MTI-related marker genes *MYB51*, *CYP71A12*, *PRX33*, and *LECRK-IX.2* in roots of wild-type and *myb36-2/sgn3-3* treated with WCS417 and flg22 (Figures 7E–7H). For all genes tested, there was a stronger response to flg22 in the endodermal barrier mutant, indicating that increased permeability of the endodermis makes roots more responsive to MAMPs. This is consistent with findings showing that flg22 could reach the inner cell types of plants with dysfunctional endodermal barriers and activate stronger expression of MTI-related marker genes (Zhou et al., 2020). The roots of the endodermal barrier mutant also produced a stronger induction of *CYP71A12* following treatment with WCS417 (6.22 times more expression compared with *myb36-2/sgn3-3* control and 3.4 times more compared with the

respective change in Col-0; Figure 7F), suggesting that the increased colonization of these roots (Figure 7D) can lead to stronger root defense responses, probably via diffusion of WCS417 MAMPs into deeper root layers.

DISCUSSION

Cell-type-specific transcriptomics reveal "hidden" root responses to WCS417

The hidden half of plants, the root system, is of crucial importance when breeding for plants that are drought tolerant or better able to grow under nutrient-limiting conditions (Rogers and Benfey, 2015; Koevoets et al., 2016). Additionally, the root surface lies at the interface between plants and beneficial soil micro-organisms, which increase plant growth and health (Lugtenberg and Kamilova, 2009; Pieterse et al., 2014; Bakker et al., 2018). Cell-type-specific transcriptomics is an approach to better understand root response to beneficial bacteria at the individual cell type level. Innovative methods have been developed to assess cell-type-specific gene expression changes. These include protoplasting-based single-cell RNA sequencing but also translating ribosome affinity purification followed by RNA sequencing, which uses nuclei rather than protoplasts for RNA extraction and consequently allows for direct snap freezing of samples (Thellmann et al., 2020; Denyer and Timmermans, 2022). Using this approach, one could circumvent potential effects of protoplasting. At the time this experiment was conducted, the relevant translating ribosome affinity purification followed by RNA sequencing transgenic reporter lines were not available. Therefore, we studied gene expression changes in five *Arabidopsis* root cell types after colonization with WCS417 using FACS (Figures 2 and 3). The total number of DEGs identified across the five cell types is approximately 10-fold greater than the number identified in the sorted whole root control. A similar increase in detection power of cell-type-specific versus whole-root transcriptomic analyses was obtained previously when examining the *Arabidopsis* root response to salt, iron deficiency, and nitrogen (Dinneny et al., 2008; Gifford et al., 2008).

We showed that the increased sensitivity can be traced to the cell-type-specific nature of the root response to WCS417. The five cell types differ in their response to WCS417 both quantitatively, with major differences in the number of DEGs, and qualitatively, with little overlap in DEGs between cell types (Figure 3). This supports previous studies on cell-type-specific gene expression changes in response to both abiotic and biotic stresses and refutes the concept of a global stress response (Dinneny et al., 2008; Gifford et al., 2008; Iyer-Pascuzzi et al., 2011; Walker et al., 2017; Rich-Griffin et al., 2020a).

Root hairs, the cortex, and the endodermis have roles in the WCS417-*Arabidopsis* interaction

The number and type of DEGs in our spatial map uncovered two interesting findings: (1) the cortex and endodermis responded most strongly to WCS417 in terms of the number of DEGs, and (2) the responsiveness of the two epidermal cell types was distinct (Figure 4). The strong response of the cortex and endodermis is surprising, as these cell types were likely not in direct contact with WCS417, which preferentially colonizes the root surface. Previous studies, however, demonstrated the ability of MAMPs to reach the cortex and the endodermis (Zhou et al., 2020) and mount MTI responses (Wyrsch et al., 2015). Also timing likely plays a role, as cell-type-specific transcriptional profiling of the *Arabidopsis* root response to flg22 showed that the epidermis responded as strongly as the cortex at 2 h post inoculation (Rich-Griffin et al., 2020a). Possibly, the epidermis responds strongly at first and downregulates its response by 2 days after inoculation, while the cortex and endodermis maintain or increase their response over that period to restrict continuous and unwanted activation of the outer cell types exposed to the microbe-rich environment. We observed enrichment of processes related to decreased cell wall biogenesis in these inner cell types specifically. This might have allowed these cells to lose volume, which is required for lateral root initiation and outgrowth (Vermeer et al., 2014; Stoeckle et al., 2018). Indeed, we observed that cell wall mutants display increased emergence of lateral roots (Supplemental Figure 6), suggesting that repression of cell wall strengthening might explain the observed increase in lateral root formation in WCS417-exposed roots (Zamioudis et al., 2013; Stringlis et al., 2018a). A time-series experiment could further elucidate the timing and magnitude of these spatially-separated responses, while future studies on the responsiveness of younger and older parts of the root to different stimuli could provide further evidence as to how roots contribute to plant homeostasis in microbe-rich and stress-abundant environments.

In addition to decreased cell wall biogenesis, we showed increased expression of genes involved in suberin biosynthesis in the endodermis (Figure 6). This was further confirmed by suberin staining, which demonstrated increased suberization of the endodermis (Figure 6). On the one hand, manipulation of suberin deposition (desuberization and resuberization) might be part of the increased lateral root emergence triggered by WCS417, since emerging lateral roots need to cross the endodermis and suberin degradation is needed for correct lateral root emergence (Ursache et al., 2021). On the other hand, suberin and the Casparian strip are essential for protecting the inner root tissues from the surrounding soil environment (Barberon, 2017). Suberin displays plasticity to nutrient stresses such as iron deficiency (Barberon et al., 2016), but it can also be modulated in response to beneficial and pathogenic members of the microbiome (Froschel et al., 2020; Salas-Gonzalez et al., 2021; Kashyap et al., 2022). It is probable that both beneficial and pathogenic micro-organisms manipulate the functioning and deposition of endodermal barriers to achieve sufficient colonization of the root and access to root-derived sugars. Indeed, previous research has shown that *Arabidopsis* activates the iron deficiency response upon root colonization by WCS417 (Verhagen et al., 2004; Zamioudis et al., 2014, 2015). This response is normally activated when plants experience a shortage of iron and results in a decreased deposition of suberin to facilitate iron uptake (Barberon et al., 2016), suggesting that WCS417 modulates nutrient availability or use within the plant. Our data further suggested that this might be a transient response during colonization, since, at 48 h after colonization, we observed increased, rather than decreased, suberization in the roots, suggesting that plants adapt to the interaction with WCS417 and re-seal the endodermis to avoid unwanted effects. This

hypothesis is supported by our experiment with the *myb36-2/sgn3-3* double mutant with dysfunctional endodermal barriers. This mutant is colonized to a higher degree by WCS417 and has elevated expression of the MTI-related marker gene *CYP71A12* compared with wild-type plants (Figure 7). Additionally, in this mutant, three of four MTI-related marker genes showed increased expression in response to flg22, further confirming the role of this barrier in MTI sensitivity and in fine-tuning growth and defense. Therefore, for an optimal interaction with WCS417, *Arabidopsis* needs a functional endodermal barrier to prevent limitless bacterial proliferation on the root.

Next, our findings indicated that root hairs could be acting as first responders to environmental signals and inform plants to adapt their growth and development to an upcoming interaction. Literature supports this, since, in other plant species, root hairs are colonization hotspots for rhizobia (Poole et al., 2018), the formation and pattern of root hairs are responsive to nutrient stresses, root hairs mediate exudation of iron-mobilizing coumarins (Robe et al., 2021), and barley mutant plants with contrasting root hair characteristics accommodate distinct root-associated microbial communities (Robertson-Albertyn et al., 2017). Interestingly, the *cpc* and *ttg1* mutants used here, despite their contrasting pattern in root hair formation, seemed unaffected in terms of WCS417 colonization but displayed less growth promotion compared with wild-type plants. It is possible that root hairs might have a prominent role in colonization by endophytes such as rhizobia or microbes affected by exudates released by root hairs, such as coumarins. As WCS417 can colonize the whole root system and remains on the root surface, root hairs might not be critical for its establishment on the root, yet this might also be a consequence of the simple, binary setup in which plant roots were solely colonized by one bacterium. We did observe that *cpc* and *ttg1* respond in a different transcriptional manner when colonized by WCS417. Thus, detailed transcriptomic analysis of root hair mutants and assessment of said mutants in natural soil conditions are pertinent questions that require our attention in the future to address their role in plant-beneficial microbe interactions.

In summary, we created a spatial map of gene expression changes induced in the *Arabidopsis* root in response to colonization by the beneficial bacterium WCS417. Our dataset uncovered localized, cell-type-specific gene expression patterns that otherwise remain hidden in global analyses of gene expression and that correspond to observed root architectural changes. We reveal a role for root hairs and endodermal barriers in the interaction between roots, WCS417, and MAMPs. Further mining of this dataset may enable to determine the spatial pattern of microbe-induced expression of genes of interest.

METHODS

Plant material and growth conditions

FACS experiment

Arabidopsis accession Columbia-0 (Col-0) and transgenic Col-0 with the -*COBRA-LIKE9*$_{pro}$*:GFP* (Brady et al., 2007a, 2007b), *WEREWOLF*$_{pro}$*:GFP* (Lee and Schiefelbein, 1999), *315*$_{pro}$*:GFP* (*AT1G09750*) (Lee et al., 2006), *SCARECROW*$_{pro}$*:GFP* (Wysocka-Diller et al., 2000), or *WOODENLEG*$_{truncated\_pro}$*:GFP* construct (Mahonen et al., 2000) were grown as described previously (Dinneny et al., 2008). Briefly, seeds were liquid sterilized in 50% bleach and stratified by incubation at 4°C for 2 days. Sterilized seeds were plated in two dense lines of three seeds thick each on nylon mesh (Nitex Cat 03-100/44, Sefar) on sterile 1 × Murashige and Skoog (MS) (Murashige and Skoog, 1962) 1% sucrose plates. Plates were sealed with Parafilm and placed vertically in long-day conditions (22°C; 16 h light, 8 h dark) for a total of 7 days.

Microscopy for suberin localization

Col-0 seeds were surface sterilized (Van Wees et al., 2013) and sown on plates containing agar-solidified Hoagland medium with 1% sucrose, and pH was adjusted to 5.5. After 2 day of stratification at 4°C, the plates were positioned vertically and transferred to a growth chamber (22°C; 10 h light, 14 h dark; light intensity 100 μmol m^{-2} s^{-1}). When 5 days old, seedlings were transferred to agar-solidified Hoagland plates without sucrose (0.75% agar) where *P. simiae* WCS417 (WCS417) was mixed in the medium based on the protocol developed by Paredes et al. (2018). After 2 days of *Arabidopsis*-WCS417 interaction, FY staining of roots was performed as described before (Lux et al., 2005; Kajala et al., 2021).

Colonization and growth-promotion experiments with root hair, cell wall integrity, and endodermal barrier mutants

Col-0 seeds and mutants in Col-0 background *myb36-2/sgn3-3* (Reyt et al., 2021), *cpc-1* and *ttg1* (Wada et al., 1997; Walker et al., 1999), and *irx9*, *irx9L*, *irx14* and *irx14L* (Wu et al., 2010) were surface sterilized and sown on agar-solidified Hoagland plates (as before). When 7 days old, seedlings, except *irx* mutants, were transferred to agar-solidified Hoagland plates with 0% sucrose where WCS417 was mixed in the medium (as before). In the case of *irx* mutants, 7-day-old seedlings were transferred to Hoagland plates with 1% sucrose, and subsequently the plants were inoculated with either WCS417 bacteria by applying 10 μl of a bacterial suspension on the root-shoot junction or a mock solution containing 10 mM $MgSO_4$. Seven days later, the shoots of the seedlings were weighed using an analytical scale, photos were taken to analyze root growth and development (via ImageJ), and colonization of WCS417 on roots was assessed (Paredes et al., 2018).

Analysis of gene expression in endodermal barrier and root hair mutants

For testing root transcriptional responses to WCS417 and flg22, plants were grown and treated based on a protocol developed by Stringlis et al. (2018a). Briefly, uniform 9-day-old seedlings were transferred from MS agar plates to six-well plates (ø 35 mm per well) containing liquid 1× MS with 0.5% sucrose, after which they were cultured for a further 7 days under the same growth conditions. One day before treatment with either WCS417 or flg22, the medium of each well was replaced with fresh 1× MS medium with 0.5% sucrose. At 6 h after treatment with WCS417 or 1 μM flg22 (GenScript), roots were flash-frozen in liquid nitrogen for downstream gene expression analysis.

WCS417 treatment

FACS experiment

Plants were inoculated with bacteria 5 days after being placed in long-day conditions using a slightly adapted version of a previously published protocol (Zamioudis et al., 2015). Briefly, rifampicin-resistant WCS417 was streaked from a frozen glycerol stock onto solid King's medium B (KB) containing 50 μg ml^{-1} rifampicin and grown at 30°C overnight. One day before plant treatment, a single colony from the plate was put in liquid KB with rifampicin and grown in a shaking incubator at 30°C overnight. The following morning, the bacterial suspension was diluted in fresh KB with rifampicin and grown in a shaker until the suspension reached an optical density at 600 nm (OD_{600}) value between 0.6 and 1.0 (OD_{600} of 1.00 is equal to 10^9 CFU ml^{-1}), after which the bacteria were washed twice with 10 mM $MgCl_2$.

To decide which bacterial concentration to add to the plants, the washed bacteria were resuspended in 10 mM $MgCl_2$ to a final density ranging from 10^1 to 10^8 CFU μl^{-1}. Two horizontal lines of either 10 μl of 10 mM $MgCl_2$ or

10 μl of one of the bacterial suspensions were applied per 1× MS 1% sucrose plate. Five-day-old Col-0 seedlings were transferred on their mesh onto these plates. Seedlings were transferred such that the roots of the seedlings were on top of the bacteria. Finally, all plates were resealed with Parafilm and left to grow in long-day conditions. At 2 and 7 days after treatment, 10 plants from each treatment were randomly picked and removed from the plate. By this time, the bacteria had formed an extensive biofilm covering the entire root, visible to the naked eye. The total number of emerged lateral roots was counted under a stereomicroscope. ImageJ was used to determine primary root length per plant from images made with a scanner.

Based on the results of this trial, we chose a density of 10^6 CFU μl^{-1}, amounting to 10^7 CFU per row of plants, for the sorting experiment (see below). Wild-type Col-0 plants and plants of each of the five transgenic lines were exposed to this bacterial density after 5 days of plant growth as described above and incubated in long-day growth conditions for an additional 2 days.

Suberin staining experiment and colonization, and assessment of growth and gene expression of endodermal and root hair mutants

For the rest of experiments, WCS417 was prepared and applied based on previously established protocols (Stringlis et al., 2018a; Paredes et al., 2018). WCS417 was cultured at 28°C on KB agar plates supplemented with 50 μg ml^{-1} of rifampicin. After 24 h of growth, cells were collected in 10 mM $MgSO_4$, washed twice with 10 mM $MgSO_4$ by centrifugation for 5 min at 5000 *g*, and finally resuspended in 10 mM $MgSO_4$. For suberin staining and growth/colonization experiments of Col-0 and mutant seedlings, WCS417 was mixed in Hoagland agar plates without sucrose in a concentration of 10^5 CFU ml^{-1}. This mix was then poured in plates and the seedlings were transferred to the plate once solidified.

For qRT-PCR gene expression analysis of Col-0 and respective mutants, WCS417 bacteria were added in each well to a final OD_{600} of 0.1 (10^8 CFU ml^{-1}).

FACS

After a total of 7 days of growth, roots were cut from the shoot with a carbon steel surgical blade. Whole roots of Col-0 destined for the unsorted control were immediately frozen in liquid nitrogen in an Eppendorf tube. For the other samples, all to be put through a cell sorter, roots were cut twice more and the root pieces from –four to six plates were collected and protoplasted as described previously (Birnbaum et al., 2003, 2005). Briefly, they were placed in a 70-μm cell strainer submerged in enzyme solution (600 mM mannitol, 2 mM $MgCl_2$, 0.1% BSA, 2 mM $CaCl_2$, 2 mM MES (2-(N-morpholino)ethanesulfonic acid), 10 mM KCl, pH 5.5 with 0.75 g cellulysin and 0.05 g pectolyase per 50 ml). Roots were mixed in the strainer at room temperature (RT) on an orbital shaker to dissociate protoplasts. After 1 h, the suspension surrounding the strainer, containing the protoplasts, plus a few roots to pull the protoplasts down, were pipetted into a 15-ml conical tube and spun at 200 *g* for 6 min at RT. The top of the supernatant was pipetted off and the remaining solution resuspended in 700 μl of the protoplasting solution without enzymes (600 mM mannitol, 2 mM $MgCl_2$, 0.1% BSA, 2 mM $CaCl_2$, 2 mM MES, 10 mM KCl, pH 5.5). This suspension was filtered successively through a 70-μm cell strainer and a 40-μm strainer. The filtrate was finally collected in a cell sorting tube and taken to the cell sorter (Astrios, Beckman Coulter) at RT.

Protoplasts sorted by the machine were collected into RLT buffer (Qiagen) with β-mercaptoethanol. The samples were immediately placed on dry ice to inhibit RNA degradation. Samples were stored at −80°C until RNA isolation.

RNA isolation and sequencing

FACS experiment

Whole-root tissue for the unsorted control was lysed by grinding with a liquid-nitrogen-cooled mortar and pestle. RNA was isolated with the RNeasy Plant Mini Kit (Qiagen) for the six unsorted whole-root samples and for six out of eight sorted whole-root samples. RNA from the remaining two sorted whole-root samples and all cell-type-enriched samples were isolated with the Micro Kit (Qiagen). RNA concentration was checked with a Qubit Fluorometer (Thermo Scientific), and RNA integrity was assessed with a Bioanalyzer (Agilent Technologies). Subsequently, RNA libraries were made from samples with RNA integrity number values above six. All libraries were made with the NEBNext Ultra RNA Library Prep Kit for Illumina (NEB). RNA for the six control unsorted (whole root) and the first six control sorted samples were poly(A) selected using Dynal Oligo-dT beads. These 12 libraries were generated using 100 ng of total RNA. The remaining libraries were generated from total RNA selected using NEBNext Oligo-dT beads. Because of limited RNA yields from some of the sorted cell populations, 50 ng of total RNA was used as starting material for all sorted library preparations. Libraries were sequenced on an Illumina HiSeq 2500 using 50 base pair single read (Duke University Sequencing Core). Three biological replicates were performed for each sample type and condition, except for the sorted control, for which we performed four biological replicates.

qRT-PCR experiment of Col-0 and mutants

For the qRT-PCR experiment, roots of Col-0 and mutants were collected in four replicates at 6 h after treatment with live WCS417 cells or flg22. Roots of untreated Col-0 and mutant seedlings were collected at the same time point (as controls). Each of the four biological replicates per treatment consisted of 10–12 pooled root systems. After harvest, root samples were snap-frozen in liquid nitrogen and stored at −80°C. *Arabidopsis* roots were homogenized using a mixer mill (Retsch) set to 30 Hz for 45 s. RNA extraction was performed with the RNeasy Plant Mini Kit (Qiagen). RNA concentration was checked with a Qubit Fluorometer (Thermo Scientific). For qRT-PCR analysis, DNase treatment, cDNA synthesis, and PCR reactions and subsequent analysis were performed as described by Stringlis et al. (2018b). Primer sequences for the reference gene *PP2AA3* and the MTI marker genes *MYB51*, *CYP71A12*, *LECRK-IX.2*, and *PRX33* are listed in Supplemental Table 15.

Data analysis

FACS analysis

The reads generated by Illumina sequencing were pseudoaligned to the TAIR10 cDNA database (Lamesch et al., 2012) using Kallisto (v0.43.0) with 100 bootstraps and default settings (Bray et al., 2016). The percentage of aligned reads is lower for the 12 samples that were poly(A) selected using Dynal Oligo-dT beads because of a high number of rRNA sequences. This is probably due to differences in the bead-selection procedure and the greater amount of RNA used as starting material. We do not expect this to interfere with our analyses, as the number of expressed genes in these samples is in the same range as previously published data in this species. The resulting transcript counts were subsequently summarized to the gene level with tximport (v1.2.0) (Soneson et al., 2015). We then assessed the number of detected expressed genes by counting the number of genes with count above 0, above 10, or with counts per million above 2. One bacteria-exposed sample enriched for trichoblasts was excluded from further analyses because of low coverage for all three of these criteria. Only genes with counts per million greater than 2 in all samples were kept for the remaining analysis. The counts per gene of the remaining samples and genes were used to generate a digital gene expression list in EdgeR (v3.16.5) (Robinson et al., 2010). A generalized linear model (glm) was fitted using a negative binomial model and quasi-likelihood dispersion estimated from the deviance with the glmQLFit function in EdgeR. DEGs were then determined by comparing the bacteria-exposed and the non-exposed samples with the glmQLFTest (FDR < 0.1; $-2 < \log_{2\ \text{fold change}}[\log_2 FC] > 2$). GO term analysis was performed in R based on the genome-wide annotation for *Arabidopsis* within org.At.tair.db (Carlson, 2019) with the program GOstats (Falcon and Gentleman, 2007).

Analysis of cell type specificity

To investigate and confirm the cell-type-specific expression of *WOL* (*AT2G01830*) and selected vasculature-specific genes *INCURVATA4*

(*AT1G52150*), *SHR* (*AT4G37650*), and *ZLL* (*AT5G43810*), we used the *Arabidopsis* single-cell root atlas and associated procedures described in Shahan et al. (2022). To support the cell type specificity of the here-described FACS dataset, we also took the top-50 marker genes per cell type from Shahan et al. (2022). Specifically, we obtained the top-50 marker genes for trichoblasts, atrichoblasts, cortical cells, endodermal cells, and vasculature cells from Shahan et al. (2022) (Supplementary Dataset 2K), and derived the corresponding TPM value for each sample in our FACS dataset. Next, we scaled each gene using the base R function "scale" across all samples and plotted the scaled TPM values for each Shahan et al. (2022) marker-based, cell-type-top-50 gene for each FACS sample type in a boxplot using the ggplot2 R *geom_boxplot* function.

Fluorescence microscopy

Approximately 20 sterilized and vernalized seeds of the $COBL9_{pro}$:*GFP*, WER_{pro}:*GFP*, 315_{pro}:*GFP*, SCR_{pro}:*GFP*, and $WOL_{truncated\_pro}$:*GFP* transgenic lines were sown on a 1× MS 1% sucrose plate and placed in long-day conditions. After 5 days, either 10^5 WCS417 cells in 10 μl of $MgCl_2$ or sterile 10 μl of $MgCl_2$ was added to each root. GFP localization was observed once per day in 5-, 6-, and 7-day-old seedlings with a 510 upright confocal microscope with a 20× objective (Zeiss).

For FY staining of suberin, Col-0 seeds were sown on Hoagland plates 1% sucrose and placed in short-day conditions. When 5 days old, seedlings were transferred in Hoagland medium without sucrose mixed with 10^5 CFU ml^{-1} WCS417. After 2 days, roots were washed in MQ, separated from the leaves, and five roots were added in each well of six-well plates and incubated in FY088 (0.01% w/v, dissolved in lactic acid) for 1 h at RT in darkness, rinsed three times with water (5 min per wash), and counter-stained with aniline blue (0.5% w/v, dissolved in water) for 1 h at RT in darkness. Roots were mounted with 50% glycerol on glass slides and kept in dark until observation. Confocal laser scanning microscopy was performed on a Zeiss LSM 700 laser scanning confocal microscope with the 20× objective and GFP filter (488-nm excitation, 500- to 550-nm emission). To quantify the suberization pattern, the distance from the root tip to the start of continuous suberization was determined with ImageJ (v1.53g).

DATA AVAILABILITY

The raw RNA sequencing read data are deposited with links to BioProject accession number PRJNA836026 in the NCBI BioProject database.

SUPPLEMENTAL INFORMATION

Supplemental information is available at *Molecular Plant Online*.

FUNDING

This research was funded in part by the Netherlands Organization of Scientific Research through ALW Topsector Grant no. 831.14.001 (E.H.V.), by a postdoctoral fellowship from the Jane Coffin Childs Memorial Fund for Medical Research (L.M.L.), by the NIH (5R01-GM-043778), the NSF (MCB-06-18304), the Gordon and Betty Moore Foundation and the Howard Hughes Medical Institute (P.N.B.), by a postdoctoral fellowship from the Research Foundation Flanders (FWO 12B8116N) (R.d.J.), by the NWO Green II Grant no. ALWGR.2017.002 (R.d.J.), the Novo Nordisk Foundation Grant no. NNF19SA0059362 (R.d.J.), the China Scholarship Council (CSC) scholarship no. 201908320054 (J.Z.), scholarship no. 202006990074 (J.Y.), the Technology Foundation Perspective Program Back2Roots grant no. 14219 (C.M.J.P.), the ERC Advanced Grant no. 269072 of the European Research Council (C.M.J.P.), and the NWO Gravitation Grant no. 024.004.014 (I.A.S. and C.M.J.).

AUTHOR CONTRIBUTIONS

Conceptualization, E.H.V., L.M.L., P.N.B., C.M.J.P., I.A.S., and R.d.J., methodology, E.H.V. and L.M.L., formal analysis, E.H.V. and R.d.J.; investigation, E.H.V., L.M.L., J.Z., J.Y., and I.A.S.; writing – original draft, E.H.V., L.M.L., C.M.J.P., I.A.S., and R.d.J.; writing – review & editing, L.M.L., P.N.B., C.M.J.P., I.A.S., and R.d.J.; visualization, E.H.V., L.M.L., J.Z., J.Y., I.A.S., and R.d.J.; funding acquisition, E.H.V., L.M.L., C.M.J.P., P.N.B., and R.d.J.

ACKNOWLEDGMENTS

The authors want to thank Niko Geldner for the *myb36-2/sgn3-3* lines, Christian Dubos for *cpc* and *ttg1* lines, Cara M. Winter for help with FACS lines microscopy, Hao Zhang for helping with the *irx* mutants experiments, and Rosa Toonen for the experiment involving suberin staining and confocal microscopy. No conflict of interest is declared.

Received: May 9, 2022
Revised: March 30, 2023
Accepted: June 1, 2023
Published: June 5, 2023

REFERENCES

Barberon, M. (2017). The endodermis as a checkpoint for nutrients. New Phytol. **213**:1604–1610.

Barberon, M., Vermeer, J.E., De Bellis, D., Wang, P., Naseer, S., Andersen, T.G., Humbel, B.M., Nawrath, C., Takano, J., Salt, D.E., et al. (2016). Adaptation of root function by nutrient-induced plasticity of endodermal differentiation. Cell **164**:447–459.

Bakker, P.A.H.M., Pieterse, C.M.J., de Jonge, R., and Berendsen, R.L. (2018). The soil-borne legacy. Cell **172**:1178–1180.

Beck, M., Wyrsch, I., Strutt, J., Wimalasekera, R., Webb, A., Boller, T., and Robatzek, S. (2014). Expression patterns of *FLAGELLIN SENSING 2* map to bacterial entry sites in plant shoots and roots. J. Exp. Bot. **65**:6487–6498.

Berendsen, R.L., Van Verk, M.C., Stringlis, I.A., Zamioudis, C., Tommassen, J., Pieterse, C.M.J., and Bakker, P.A.H.M. (2015). Unearthing the genomes of plant-beneficial *Pseudomonas* model strains WCS358, WCS374 and WCS417. BMC Genom. **16**:539.

Birnbaum, K., Jung, J.W., Wang, J.Y., Lambert, G.M., Hirst, J.A., Galbraith, D.W., and Benfey, P.N. (2005). Cell type-specific expression profiling in plants via cell sorting of protoplasts from fluorescent reporter lines. Nat. Methods **2**:615–619.

Birnbaum, K., Shasha, D.E., Wang, J.Y., Jung, J.W., Lambert, G.M., Galbraith, D.W., and Benfey, P.N. (2003). A gene expression map of the *Arabidopsis* root. Science **302**:1956–1960.

Brady, S.M., Orlando, D.A., Lee, J.Y., Wang, J.Y., Koch, J., Dinneny, J.R., Mace, D., Ohler, U., and Benfey, P.N. (2007a). A high-resolution root spatiotemporal map reveals dominant expression patterns. Science **318**:801–806.

Brady, S.M., Song, S., Dhugga, K.S., Rafalski, J.A., and Benfey, P.N. (2007b). Combining expression and comparative evolutionary analysis. The COBRA gene family. Plant Physiol. **143**:172–187.

Carlson, M. (2019). org.At.tair.db: Genome wide annotation for Arabidopsis (R package version 3.8.2).

Bray, N.L., Pimentel, H., Melsted, P., and Pachter, L. (2016). Near-optimal probabilistic RNA-seq quantification. Nat Biotechnol **34**:525–527.

Colaianni, N.R., Parys, K., Lee, H.S., Conway, J.M., Kim, N.H., Edelbacher, N., Mucyn, T.S., Madalinski, M., Law, T.F., Jones, C.D., et al. (2021). A complex immune response to flagellin epitope variation in commensal communities. Cell Host Microbe **29**:635–649.e9.

Contreras-Cornejo, H.A., Macías-Rodríguez, L., Cortés-Penagos, C., and López-Bucio, J. (2009). *Trichoderma virens*, a plant beneficial fungus, enhances biomass production and promotes lateral root growth through an auxin-dependent mechanism in Arabidopsis. Plant Physiol. **149**:1579–1592.

Denyer, T., and Timmermans, M.C.P. (2022). Crafting a blueprint for single-cell RNA sequencing. Trends Plant Sci. **27**:92–103.

Dinneny, J.R., Long, T.A., Wang, J.Y., Jung, J.W., Mace, D., Pointer, S., Barron, C., Brady, S.M., Schiefelbein, J., and Benfey, P.N. (2008). Cell identity mediates the response of *Arabidopsis* roots to abiotic stress. Science **320**:942–945.

Dolan, L., Janmaat, K., Willemsen, V., Linstead, P., Poethig, S., Roberts, K., and Scheres, B. (1993). Cellular organisation of the *Arabidopsis thaliana* root. Development **119**:71–84.

Du, Y., and Scheres, B. (2018). Lateral root formation and the multiple roles of auxin. J. Exp. Bot. **69**:155–167.

Falcon, S., and Gentleman, R. (2007). Using GOstats to test gene lists for GO term association. Bioinformatics **23**:257–258.

Froschel, C., Komorek, J., Attard, A., Marsell, A., Lopez-Arboleda, W.A., Le Berre, J., Wolf, E., Geldner, N., Waller, F., Korte, A., et al. (2020). Plant roots employ cell-layer-specific programs to respond to pathogenic and beneficial microbes. Cell Host Microbe **29**:299–310.

Geldner, N. (2013). The endodermis. Annu. Rev. Plant Biol. **64**:531–558.

Gifford, M.L., Dean, A., Gutierrez, R.A., Coruzzi, G.M., and Birnbaum, K.D. (2008). Cell-specific nitrogen responses mediate developmental plasticity. Proc. Natl. Acad. Sci. USA **105**:803–808.

Gilroy, S., and Jones, D.L. (2000). Through form to function: root hair development and nutrient uptake. Trends Plant Sci. **5**:56–60.

Hacquard, S., Spaepen, S., Garrido-Oter, R., and Schulze-Lefert, P. (2017). Interplay between innate immunity and the plant microbiota. Annu. Rev. Phytopathol. **55**:565–589.

Harbort, C.J., Hashimoto, M., Inoue, H., Niu, Y., Guan, R., Rombolà, A.D., Kopriva, S., Voges, M.J.E.E.E., Sattely, E.S., Garrido-Oter, R., and Schulze-Lefert, P. (2020). Root-secreted coumarins and the microbiota interact to improve iron nutrition in Arabidopsis. Cell Host Microbe **28**:825–837.e6.

Iyer-Pascuzzi, A.S., Jackson, T., Cui, H., Petricka, J.J., Busch, W., Tsukagoshi, H., and Benfey, P.N. (2011). Cell identity regulators link development and stress responses in the Arabidopsis root. Dev. Cell **21**:770–782.

Kajala, K., Gouran, M., Shaar-Moshe, L., Mason, G.A., Rodriguez-Medina, J., Kawa, D., Pauluzzi, G., Reynoso, M., Canto-Pastor, A., Manzano, C., et al. (2021). Innovation, conservation, and repurposing of gene function in root cell type development. Cell **184**:5070.

Kámán-Tóth, E., Dankó, T., Gullner, G., Bozsó, Z., Palkovics, L., and Pogány, M. (2019). Contribution of cell wall peroxidase- and NADPH oxidase-derived reactive oxygen species to *Alternaria brassicicola*-induced oxidative burst in *Arabidopsis*. Mol. Plant Pathol. **20**:485–499.

Kashyap, A., Jiménez-Jiménez, Á.L., Zhang, W., Capellades, M., Srinivasan, S., Laromaine, A., Serra, O., Figueras, M., Rencoret, J., Gutiérrez, A., et al. (2022). Induced ligno-suberin vascular coating and tyramine-derived hydroxycinnamic acid amides restrict *Ralstonia solanacearum* colonization in resistant tomato. New Phytol. **234**:1411–1429.

Kashyap, A., Planas-Marquès, M., Capellades, M., Valls, M., and Coll, N.S. (2021). Blocking intruders: inducible physico-chemical barriers against plant vascular wilt pathogens. J. Exp. Bot. **72**:184–198.

Koevoets, I.T., Venema, J.H., Elzenga, J.T.M., and Testerink, C. (2016). Roots withstanding their environment: exploiting root system architecture responses to abiotic stress to improve crop tolerance. Front. Plant Sci. **7**:1335.

Kosma, D.K., Murmu, J., Razeq, F.M., Santos, P., Bourgault, R., Molina, I., and Rowland, O. (2014). AtMYB41 activates ectopic suberin synthesis and assembly in multiple plant species and cell types. Plant J. **80**:216–229.

Lamesch, P., Berardini, T.Z., Li, D., Swarbreck, D., Wilks, C., Sasidharan, R., Muller, R., Dreher, K., Alexander, D.L., Garcia-Hernandez, M., Karthikeyan, A.S., Lee, C.H., Nelson, W.D., Ploetz, L., Singh, S., Wensel, A., and Huala, E. (2012). The Arabidopsis Information Resource (TAIR): improved gene annotation and new tools. Nucleic Acids Res **40**:D1202–D1210.

Lashbrooke, J., Cohen, H., Levy-Samocha, D., Tzfadia, O., Panizel, I., Zeisler, V., Massalha, H., Stern, A., Trainotti, L., Schreiber, L., et al. (2016). MYB107 and MYB9 homologs regulate suberin deposition in angiosperms. Plant Cell **28**:2097–2116.

Lee, J.Y., Colinas, J., Wang, J.Y., Mace, D., Ohler, U., and Benfey, P.N. (2006). Transcriptional and posttranscriptional regulation of transcription factor expression in *Arabidopsis* roots. Proc. Natl. Acad. Sci. USA **103**:6055–6060.

Lee, M.M., and Schiefelbein, J. (1999). WEREWOLF, a MYB-related protein in *Arabidopsis*, is a position-dependent regulator of epidermal cell patterning. Cell **99**:473–483.

Li, X., Zeng, R., and Liao, H. (2016). Improving crop nutrient efficiency through root architecture modifications. J. Integr. Plant Biol. **58**:193–202.

López-Bucio, J., Campos-Cuevas, J.C., Hernández-Calderón, E., Velásquez-Becerra, C., Farías-Rodríguez, R., Macías-Rodríguez, L.I., and Valencia-Cantero, E. (2007). *Bacillus megaterium* rhizobacteria promote growth and alter root-system architecture through an auxin- and ethylene-independent signaling mechanism in *Arabidopsis thaliana*. Mol. Plant Microbe Interact. **20**:207–217.

Lugtenberg, B., and Kamilova, F. (2009). Plant-growth-promoting rhizobacteria. Annu. Rev. Microbiol. **63**:541–556.

Luo, X., Xu, N., Huang, J., Gao, F., Zou, H., Boudsocq, M., Coaker, G., and Liu, J. (2017). A lectin receptor-like kinase mediates pattern-triggered salicylic acid signaling. Plant Physiol. **174**:2501–2514.

Lux, A., Morita, S., Abe, J., and Ito, K. (2005). An improved method for clearing and staining free-hand sections and whole-mount samples. Ann. Bot. **96**:989–996.

Ma, K.W., Niu, Y., Jia, Y., Ordon, J., Copeland, C., Emonet, A., Geldner, N., Guan, R., Stolze, S.C., Nakagami, H., et al. (2021). Coordination of microbe-host homeostasis by crosstalk with plant innate immunity. Nat. Plants **7**:814–825.

Mähönen, A.P., Bonke, M., Kauppinen, L., Riikonen, M., Benfey, P.N., and Helariutta, Y. (2000). A novel two-component hybrid molecule regulates vascular morphogenesis of the Arabidopsis root. Genes Dev. **14**:2938–2943.

Malamy, J.E., and Benfey, P.N. (1997). Organization and cell differentiation in lateral roots of *Arabidopsis thaliana*. Development **124**:33–44.

Millet, Y.A., Danna, C.H., Clay, N.K., Songnuan, W., Simon, M.D., Werck-Reichhart, D., and Ausubel, F.M. (2010). Innate immune responses activated in *Arabidopsis* roots by microbe-associated molecular patterns. Plant Cell **22**:973–990.

Möller, B.K., Xuan, W., and Beeckman, T. (2017). Dynamic control of lateral root positioning. Curr. Opin. Plant Biol. **35**:1–7.

Motte, H., Vanneste, S., and Beeckman, T. (2019). Molecular and environmental regulation of root development. Annu. Rev. Plant Biol. **70**:465–488.

Murashige, T., and Skoog, F. (1962). A revised medium for rapid growth and bio assays with tobacco tissue cultures. Physiol. Plant. **15**:473–497.

Naseer, S., Lee, Y., Lapierre, C., Franke, R., Nawrath, C., and Geldner, N. (2012). Casparian strip diffusion barrier in *Arabidopsis* is made of a lignin polymer without suberin. Proc. Natl. Acad. Sci. USA **109**:10101–10106.

Ogawa, M., Kay, P., Wilson, S., and Swain, S.M. (2009). ARABIDOPSIS DEHISCENCE ZONE POLYGALACTURONASE1 (ADPG1), ADPG2, and QUARTET2 are polygalacturonases required for cell separation during reproductive development in *Arabidopsis*. Plant Cell **21**:216–233.

Ötvös, K., and Benková, E. (2017). Spatiotemporal mechanisms of root branching. Curr. Opin. Genet. Dev. **45**:82–89.

Panikashvili, D., Shi, J.X., Bocobza, S., Franke, R.B., Schreiber, L., and Aharoni, A. (2010). The *Arabidopsis* DSO/ABCG11 transporter affects cutin metabolism in reproductive organs and suberin in roots. Mol. Plant **3**:563–575.

Herrera Paredes, S., Gao, T., Law, T.F., Finkel, O.M., Mucyn, T., Teixeira, P.J.P.L., Salas González, I., Feltcher, M.E., Powers, M.J., Shank, E.A., et al. (2018). Design of synthetic bacterial communities for predictable plant phenotypes. PLoS Biol. **16**:e2003962.

Pascale, A., Proietti, S., Pantelides, I.S., and Stringlis, I.A. (2019). Modulation of the root microbiome by plant molecules: the basis for targeted disease suppression and plant growth promotion. Front. Plant Sci. **10**:1741.

Petricka, J.J., Winter, C.M., and Benfey, P.N. (2012). Control of *Arabidopsis* root development. Annu. Rev. Plant Biol. **63**:563–590.

Pieterse, C.M.J., Berendsen, R.L., de Jonge, R., Stringlis, I.A., Van Dijken, A.J.H., Van Pelt, J.A., Van Wees, S.C.M., Yu, K., Zamioudis, C., and Bakker, P.A.H.M. (2021). *Pseudomonas simiae* WCS417: star track of a model beneficial rhizobacterium. Plant Soil **461**:245–263.

Pieterse, C.M., van Wees, S.C., Hoffland, E., Van Pelt, J.A., and Van Loon, L.C. (1996). Systemic resistance in Arabidopsis induced by biocontrol bacteria is independent of salicylic acid accumulation and pathogenesis-related gene expression. Plant Cell **8**:1225–1237.

Pieterse, C.M.J., Zamioudis, C., Berendsen, R.L., Weller, D.M., Van Wees, S.C.M., and Bakker, P.A.H.M. (2014). Induced systemic resistance by beneficial microbes. Annu. Rev. Phytopathol. **52**:347–375.

Poole, P., Ramachandran, V., and Terpolilli, J. (2018). Rhizobia: from saprophytes to endosymbionts. Nat. Rev. Microbiol. **16**:291–303.

Reyt, G., Ramakrishna, P., Salas-González, I., Fujita, S., Love, A., Tiemessen, D., Lapierre, C., Morreel, K., Calvo-Polanco, M., Flis, P., et al. (2021). Two chemically distinct root lignin barriers control solute and water balance. Nat. Commun. **12**:2320.

Rich-Griffin, C., Eichmann, R., Reitz, M.U., Hermann, S., Woolley-Allen, K., Brown, P.E., Wiwatdirekkul, K., Esteban, E., Pasha, A., Kogel, K.H., et al. (2020a). Regulation of cell type-specific immunity networks in *Arabidopsis* roots. Plant Cell **32**:2742–2762.

Rich-Griffin, C., Stechemesser, A., Finch, J., Lucas, E., Ott, S., and Schäfer, P. (2020b). Single-cell transcriptomics: a high-resolution avenue for plant functional genomics. Trends Plant Sci. **25**:186–197.

Robe, K., Conejero, G., Gao, F., Lefebvre-Legendre, L., Sylvestre-Gonon, E., Rofidal, V., Hem, S., Rouhier, N., Barberon, M., Hecker, A., et al. (2021). Coumarin accumulation and trafficking in *Arabidopsis thaliana*: a complex and dynamic process. New Phytol. **229**:2062–2079.

Robertson-Albertyn, S., Alegria Terrazas, R., Balbirnie, K., Blank, M., Janiak, A., Szarejko, I., Chmielewska, B., Karcz, J., Morris, J., Hedley, P.E., et al. (2017). Root hair mutations displace the barley rhizosphere microbiota. Front. Plant Sci. **8**:1094.

Robinson, M.D., McCarthy, D.J., and Smyth, G.K. (2010). edgeR: a Bioconductor package for differential expression analysis of digital gene expression data. Bioinformatics **26**:139–140.

Rogers, E.D., and Benfey, P.N. (2015). Regulation of plant root system architecture: implications for crop advancement. Curr. Opin. Biotechnol. **32**:93–98.

Ryan, E., Steer, M., and Dolan, L. (2001). Cell biology and genetics of root hair formation in *Arabidopsis thaliana*. Protoplasma **215**:140–149.

Salas-González, I., Reyt, G., Flis, P., Custódio, V., Gopaulchan, D., Bakhoum, N., Dew, T.P., Suresh, K., Franke, R.B., Dangl, J.L., et al. (2021). Coordination between microbiota and root endodermis supports plant mineral nutrient homeostasis. Science **371**:eabd0695.

Shahan, R., Hsu, C.W., Nolan, T.M., Cole, B.J., Taylor, I.W., Greenstreet, L., Zhang, S., Afanassiev, A., Vlot, A.H.C., Schiebinger, G., et al. (2022). A single-cell *Arabidopsis* root atlas reveals developmental trajectories in wild-type and cell identity mutants. Dev. Cell **57**:543–560.e9.

Shahzad, Z., and Amtmann, A. (2017). Food for thought: how nutrients regulate root system architecture. Curr. Opin. Plant Biol. **39**:80–87.

Shukla, V., Han, J.P., Cléard, F., Lefebvre-Legendre, L., Gully, K., Flis, P., Berhin, A., Andersen, T.G., Salt, D.E., Nawrath, C., and Barberon, M. (2021). Suberin plasticity to developmental and exogenous cues is regulated by a set of MYB transcription factors. Proc. Natl. Acad. Sci. USA **118**. e2101730118.

Soneson, C., Love, M.I., and Robinson, M.D. (2015). Differential analyses for RNA-seq: transcript-level estimates improve gene-level inferences. F1000Res **4**:1521.

Stassen, M.J.J., Hsu, S.-H., Pieterse, C.M.J., and Stringlis, I.A. (2021). Coumarin communication along the microbiome–root–shoot axis. Trends Plant Sci. **26**:169–183.

Stoeckle, D., Thellmann, M., and Vermeer, J.E. (2018). Breakout-lateral root emergence in *Arabidopsis thaliana*. Curr. Opin. Plant Biol. **41**:67–72.

Stringlis, I.A., Proietti, S., Hickman, R., Van Verk, M.C., Zamioudis, C., and Pieterse, C.M.J. (2018a). Root transcriptional dynamics induced by beneficial rhizobacteria and microbial immune elicitors reveal signatures of adaptation to mutualists. Plant J. **93**:166–180.

Stringlis, I.A., Yu, K., Feussner, K., de Jonge, R., Van Bentum, S., Van Verk, M.C., Berendsen, R.L., Bakker, P.A.H.M., Feussner, I., and Pieterse, C.M.J. (2018b). MYB72-dependent coumarin exudation shapes root microbiome assembly to promote plant health. Proc. Natl. Acad. Sci. USA **115**:E5213–E5222.

Teixeira, P.J.P.L., Colaianni, N.R., Law, T.F., Conway, J.M., Gilbert, S., Li, H., Salas-González, I., Panda, D., Del Risco, N.M., Finkel, O.M., et al. (2021). Specific modulation of the root immune system by a community of commensal bacteria. Proc. Natl. Acad. Sci. USA **118**. e2100678118.

Teixeira, P.J.P., Colaianni, N.R., Fitzpatrick, C.R., and Dangl, J.L. (2019). Beyond pathogens: microbiota interactions with the plant immune system. Curr. Opin. Microbiol. **49**:7–17.

Thellmann, M., Andersen, T.G., and Vermeer, J.E. (2020). Translating ribosome affinity purification (TRAP) to investigate *Arabidopsis thaliana* root development at a cell type-specific scale. J. Vis. Exp.

Ursache, R., De Jesus Vieira Teixeira, C., Dénervaud Tendon, V., Gully, K., De Bellis, D., Schmid-Siegert, E., Grube Andersen, T., Shekhar, V., Calderon, S., Pradervand, S., et al. (2021). GDSL-domain proteins have key roles in suberin polymerization and degradation. Nat. Plants **7**:353–364.

Vacheron, J., Desbrosses, G., Bouffaud, M.L., Touraine, B., Moënne-Loccoz, Y., Muller, D., Legendre, L., Wisniewski-Dyé, F., and Prigent-Combaret, C. (2013). Plant growth-promoting rhizobacteria and root system functioning. Front. Plant Sci. **4**:356.

Vacheron, J., Desbrosses, G., Renoud, S., Padilla, R., Walker, V., Muller, D., and Prigent-Combaret, C. (2018). Differential contribution of plant-beneficial functions from *Pseudomonas*

kilonensis F113 to root system architecture alterations in *Arabidopsis thaliana* and *Zea mays*. Mol. Plant Microbe Interact. **31**:212–223.

Van den Berg, C., Willemsen, V., Hage, W., Weisbeek, P., and Scheres, B. (1995). Cell fate in the *Arabidopsis* root meristem determined by directional signalling. Nature **378**:62–65.

Van Wees, S.C.M., Van Pelt, J.A., Bakker, P.A.H.M., and Pieterse, C.M.J. (2013). Bioassays for assessing jasmonate-dependent defenses triggered by pathogens, herbivorous insects, or beneficial rhizobacteria. Methods Mol. Biol. **1011**:35–49.

Verbon, E.H., and Liberman, L.M. (2016). Beneficial microbes affect endogenous mechanisms controlling root development. Trends Plant Sci. **21**:218–229.

Verhagen, B.W.M., Glazebrook, J., Zhu, T., Chang, H.S., Van Loon, L.C., and Pieterse, C.M.J. (2004). The transcriptome of rhizobacteria-induced systemic resistance in *Arabidopsis*. Mol. Plant Microbe Interact. **17**:895–908.

Vermeer, J.E.M., von Wangenheim, D., Barberon, M., Lee, Y., Stelzer, E.H.K., Maizel, A., and Geldner, N. (2014). A spatial accommodation by neighboring cells is required for organ initiation in *Arabidopsis*. Science **343**:178–183.

Vishwanath, S.J., Delude, C., Domergue, F., and Rowland, O. (2015). Suberin: biosynthesis, regulation, and polymer assembly of a protective extracellular barrier. Plant Cell Rep. **34**:573–586.

Vissenberg, K., Claeijs, N., Balcerowicz, D., and Schoenaers, S. (2020). Hormonal regulation of root hair growth and responses to the environment in Arabidopsis. J. Exp. Bot. **71**:2412–2427.

Wachsman, G., Sparks, E.E., and Benfey, P.N. (2015). Genes and networks regulating root anatomy and architecture. New Phytol. **208**:26–38.

Wada, T., Tachibana, T., Shimura, Y., and Okada, K. (1997). Epidermal cell differentiation in *Arabidopsis* determined by a Myb homolog, CPC. Science **277**:1113–1116.

Walker, A.R., Davison, P.A., Bolognesi-Winfield, A.C., James, C.M., Srinivasan, N., Blundell, T.L., Esch, J.J., Marks, M.D., and Gray, J.C. (1999). The *TRANSPARENT TESTA GLABRA1* locus, which regulates trichome differentiation and anthocyanin biosynthesis in *Arabidopsis*, encodes a WD40 repeat protein. Plant Cell **11**:1337–1350.

Walker, L., Boddington, C., Jenkins, D., Wang, Y., Grønlund, J.T., Hulsmans, J., Kumar, S., Patel, D., Moore, J.D., Carter, A., et al. (2017). Root architecture shaping by the environment is orchestrated by dynamic gene expression in space and time. Plant Cell **29**:2393–2412.

Wu, A.M., Hörnblad, E., Voxeur, A., Gerber, L., Rihouey, C., Lerouge, P., and Marchant, A. (2010). Analysis of the Arabidopsis *IRX9*/*IRX9-L* and *IRX14*/*IRX14-L* pairs of glycosyltransferase genes reveals critical contributions to biosynthesis of the hemicellulose glucuronoxylan. Plant Physiol. **153**:542–554.

Wyrsch, I., Domínguez-Ferreras, A., Geldner, N., and Boller, T. (2015). Tissue-specific FLAGELLIN-SENSING 2 (FLS2) expression in roots restores immune responses in Arabidopsis *fls2* mutants. New Phytol. **206**:774–784.

Wysocka-Diller, J.W., Helariutta, Y., Fukaki, H., Malamy, J.E., and Benfey, P.N. (2000). Molecular analysis of SCARECROW function reveals a radial patterning mechanism common to root and shoot. Development **127**:595–603.

Yadav, V., Molina, I., Ranathunge, K., Castillo, I.Q., Rothstein, S.J., and Reed, J.W. (2014). ABCG transporters are required for suberin and pollen wall extracellular barriers in *Arabidopsis*. Plant Cell **26**:3569–3588.

Yu, K., Pieterse, C.M.J., Bakker, P.A.H.M., and Berendsen, R.L. (2019a). Beneficial microbes going underground of root immunity. Plant Cell Environ. **42**:2860–2870.

Yu, K., Liu, Y., Tichelaar, R., Savant, N., Lagendijk, E., van Kuijk, S.J.L., Stringlis, I.A., van Dijken, A.J.H., Pieterse, C.M.J., Bakker, P.A.H.M., et al. (2019b). Rhizosphere-associated *Pseudomonas* suppress local root immune responses by gluconic acid-mediated lowering of environmental pH. Curr. Biol. **29**:3913–3920.e4.

Zamioudis, C., Hanson, J., and Pieterse, C.M.J. (2014). β-Glucosidase BGLU42 is a MYB72-dependent key regulator of rhizobacteria-induced systemic resistance and modulates iron deficiency responses in Arabidopsis roots. New Phytol. **204**:368–379.

Zamioudis, C., Korteland, J., Van Pelt, J.A., Van Hamersveld, M., Dombrowski, N., Bai, Y., Hanson, J., Van Verk, M.C., Ling, H.Q., Schulze-Lefert, P., and Pieterse, C.M.J. (2015). Rhizobacterial volatiles and photosynthesis-related signals coordinate *MYB72* expression in Arabidopsis roots during onset of induced systemic resistance and iron-deficiency responses. Plant J. **84**:309–322.

Zamioudis, C., Mastranesti, P., Dhonukshe, P., Blilou, I., and Pieterse, C.M.J. (2013). Unraveling root developmental programs initiated by beneficial *Pseudomonas* spp. bacteria. Plant Physiol. **162**:304–318.

Zhou, F., Emonet, A., Dénervaud Tendon, V., Marhavy, P., Wu, D., Lahaye, T., and Geldner, N. (2020). Co-incidence of damage and microbial patterns controls localized immune responses in roots. Cell **180**:440–453.e18.